© 2021. Published by The Company of Biologists Ltd | Journal of Cell Science (2021) 134, jcs258905. doi:10.1242/jcs.258905

RESEARCH ARTICLE

Cooperation of membrane-translocated syntaxin4 and basement membrane for dynamic mammary epithelial morphogenesis

Yuina Hirose[1] and Yohei Hirai[1,2,*]

ABSTRACT

Mammary epithelia undergo dramatic morphogenesis after puberty. During pregnancy, luminal epithelial cells in ductal trees are arranged to form well-polarized cystic structures surrounded by a myoepithelial cell layer, an active supplier of the basement membrane (BM). Here, we identified a novel regulatory mechanism involved in this process by using a reconstituted BM-based three-dimensional culture and aggregates of a model mouse cell line, EpH4, that had either been manipulated for inducible expression of the t-SNARE protein syntaxin4 in intact or signal peptide-connected forms, or that were genetically deficient in syntaxin4. We found that cells extruded syntaxin4 upon stimulation with the lactogenic hormone prolactin, which in turn accelerated the turnover of E-cadherin. In response to extracellular expression of syntaxin4, cell populations that were less affected by the BM actively migrated and integrated into the cell layer facing the BM. Concurrently, the BM-facing cells, which were simultaneously stimulated with syntaxin4 and BM, acquired unique epithelial characteristics to undergo dramatic cellular arrangement for cyst formation. These results highlight the importance of the concerted action of extracellular syntaxin4 extruded in response to the lactogenic hormone and BM components in epithelial morphogenesis.

KEY WORDS: Mammary gland, Syntaxin4, Epithelial morphogenesis, Epimorphin, Basement membrane, Epithelial–mesenchymal transition

INTRODUCTION

Epithelial morphogenesis is an important biological process for building tissue-specific epithelial architectures, whereby epithelial cells are assembled into three-dimensional (3D) structures composed of well-polarized epithelial sheets in which cells are tightly connected by several junctional apparatuses. In this process, an array of systemic signaling factors and extracellular matrix proteins coordinately and spatiotemporally regulate intercellular junctional components connected to cytoskeletons, creating mechanical forces to produce a 3D configuration of the epithelial cell sheets (Friedl and Mayor, 2017; Roignot et al., 2013). Although active epithelial morphogenesis occurs in several tissues during embryogenesis, this process is accompanied by cellular differentiation and is substantially irreversible. In contrast, the postnatal mammary gland is unique: fully differentiated epithelial cells undergo morphogenesis, which is accompanied by their prominent cellular arrangement under the strict control of lactogenic hormones (Macias and Hinck, 2012; Paine and Lewis, 2017). Thus, the gestation-induced morphological changes in the mammary epithelia are considered one of the most relevant models for understanding the molecular basis of epithelial morphogenesis (Ivanova et al., 2021; Shamir and Ewald, 2015).

In the pubertal mammary gland, luminal epithelial cells form single-layered tubes in primary ducts and side branches, the tips of which are often occupied by piled-up cells. In virgin mammary glands, they also exist as stratified aggregates at the end of elongating ducts termed terminal end buds (TEBs). Upon stimulation with lactogenic hormones, however, they undergo a dramatic cellular arrangement to actively form lobular structures comprising well-polarized cysts called acini or alveoli (Brisken and O'Malley, 2010; Macias and Hinck, 2012; Sternlicht et al., 2006). During this morphogenic process, all the luminal epithelial cells in the ducts and the outermost cells in the stratified ductal tips are surrounded by myoepithelial cells that actively produce major basement membrane (BM) components (Gudjonsson et al., 2005; Paine and Lewis, 2017). Moreover, these luminal cells are often in direct contact with BM components that lie outside the myoepithelial cell layer (Vidi et al., 2013). Focusing on the characteristics of lumen formation, three compelling mechanisms have been proposed: (1) apoptotic elimination of specific cell populations (Martín-Belmonte et al., 2008), referred to as the cavitation model (Debnath and Brugge, 2005); (2) expansion of apical cargo trafficking sites between cells as a result of coordinated cell division and polarization (Bryant et al., 2010); and (3) fusion of microlumens by hydraulic fracturing of cell–cell contacts (Dumortier et al., 2019). Recently, Neumann et al. clearly showed that apoptosis is not involved in mammary lumen formation (Neumann et al., 2018); however, a causal cue for the hormone-dependent quick cellular arrangement, as well as its regulatory mechanism in the mammary epithelia, remains elusive.

From a mechanistic point of view, the spatial epithelial–mesenchymal transition (EMT), which is accompanied by a reduction in polarity and intercellular adhesion in certain cell populations, has been suggested to be a leading cause of collective cell migration (Campbell and Casanova, 2016; Ewald et al., 2012). So far, the plausible regulators of the local EMT process include insoluble BM components; their impacts on the cells vary depending on the position in the tissue (Ewald et al., 2012). Indeed, epithelial cells are known to exhibit anchorage-dependent behaviors (Martín-Belmonte et al., 2008), and those adhering directly to the BM exhibit profound epithelial characteristics, such as enhanced cell–cell adhesion, decreased motility and stronger polarity (Bryant et al., 2014; Chen et al., 2013). In fact, cells situated

[1]Department of Biomedical Chemistry, Graduate School of Science and Technology, Kwansei Gakuin University, 2-1, Gakuen, Sanda 669-1337, Japan. [2]Department of Biomedical Sciences, Graduate School of Biological and Environmental Sciences, Kwansei Gakuin University, 2-1, Gakuen, Sanda 669-1337, Japan.

*Author for correspondence (y-hirai@kwansei.ac.jp)

Y. Hirai, 0000-0002-9652-5412

Handling Editor: Andrew Ewald
Received 13 May 2021; Accepted 18 October 2021

Journal of Cell Science (2021) 134, jcs258905. doi:10.1242/jcs.258905

within the TEB, a location that is substantially free from the effects of the BM, frequently show reduced intercellular adhesion, thereby potentially rearranging and exchanging their positions even in the absence of hormonal stimuli (Ewald et al., 2008, 2012; Hinck and Silberstein, 2005).

E-cadherin (also known as CDH1), an abundantly expressed intercellular adhesion molecule in mammary epithelia, is a key element responsible for the arrangement and maintenance of organized epithelial structures throughout their developmental stages. It is well known that functional ablation or downregulation of this molecule is accompanied by increased EMT-like cell behavior, and vice versa (Lamouille et al., 2014). In addition, E-cadherin-mediated adhesion often influences signaling pathways and regulates several genes involved in cell survival and proliferation (Shamir and Ewald, 2015). E-cadherin interacts with actin filaments or microtubules via catenins, its cytoplasmic binding partners, or via a member of the calmodulin-regulated spectrin-associated proteins (CAMSAPs), CAMSAP3 (Meng et al., 2008; Takeichi, 2014). While a number of studies have identified molecular elements that hamper E-cadherin-mediated intercellular adhesion, most of them target cytoplasmic junctions between E-cadherin and epithelial cytoskeletons (Fukata et al., 1999; Kuroda et al., 1998). We recently reported a direct interaction between the extracellular domain of E-cadherin and specific plasmalemmal syntaxins at the cell surface, which severely affected E-cadherin functions (Hirose et al., 2018).

Syntaxins are t-SNARE proteins that mediate intravesicular fusion in the cytoplasm. Among syntaxins, syntaxin2 (also known as epimorphin) and syntaxin4 temporally translocate across the cell membrane in response to external stimuli and subsequently execute their latent morphogenic and differentiation-inducing functions in several cell types (Hagiwara-Chatani et al., 2017; Kadono et al., 2015; Okugawa and Hirai, 2008; Radisky et al., 2009). Given that their extracellular exposure occurs without the requirement of a time-consuming transcription and translation process, the effect of their morphogenic actions is thought to be very quick and sensitive. Using a mammary epithelial cell line, SCp2, we have shown previously that certain cell populations extrude syntaxin4 upon stimulation with the lactogenic hormone, prolactin, which in turn perturbs E-cadherin function and propagates EMT-like signals. Consistently, the local presence of extracellular syntaxin4 in Scp2 aggregates leads to asymmetric tissue organization in collagen gels (Hirose et al., 2018). In contrast, another study using the same cell line cultured on plastic has shown that the effect of syntaxin4 is possibly deregulated by an insoluble BM component, laminin-111, as a consequence of direct intermolecular interactions between them (Shirai et al., 2017).

In the present study, we analyzed the functional relationship between prolactin-provoked extracellular syntaxin4 and BM components in the spatial cellular arrangement of murine mammary epithelial cells, and revealed that the spatiotemporal coordination of extruded syntaxin4 and BM components could play a key role in mammary epithelial morphogenesis.

RESULTS

Expression of syntaxin4 in the mammary gland

Luminal epithelial cells in mammary glands undergo stage-specific morphogenesis under hormonal control. For example, those in the pubertal period gradually transform into elongating ducts with side branches, the tips of which often exhibit stratified structures. In young mice, the tips of the elongating ductal tree exhibit unique TEB structures that function as a platform for subsequent morphogenesis. In contrast, those after a gestational period are actively rearranged to build up lobular structures, comprising single-layered epithelial cysts surrounded by a myoepithelial cell layer, which gradually inflates and exhibits clear apicobasal polarity for milk secretion. Syntaxin4 was detected in all the cellular compartments regardless of the developmental stage, including luminal epithelial, myoepithelial, fibroblastic and adipocytic cells. At the tip of a side branch in the pubertal gland (at 7 weeks of age), all multilayered luminal epithelial cells expressed syntaxin4 at the cell membrane in an apolar fashion. In contrast, single-layered luminal epithelial cells in the alveoli of a lactating gland expressed this molecule at the basolateral membrane (Fig. 1A). Immunostaining of luminal epithelial cells cultured with the lactogenic hormone prolactin revealed membrane translocation and extracellular expression of syntaxin4 in a subpopulation of cells (Fig. 1A).

Prolactin provokes membrane translocation of syntaxin4, which instructs dynamic cellular arrangements

Given that the non-tumorigenic murine mammary epithelial cell line EpH4 reportedly retains hormonal responses, morphogenic potential and clear apicobasal polarity, we next tested whether these cells also extruded endogenous syntaxin4 under lactogenic conditions. As observed in the primary cells, the extracellular expression of syntaxin4 upon treatment with prolactin was obvious in some EpH4 cells (Fig. 1B), suggesting that EpH4 cells are a useful model system to define the role of syntaxin4. We next investigated possible changes in 3D cell behaviors upon alteration of the amount of extracellular syntaxin4 provoked by treatment with prolactin. To this end, we generated EpH4 cells deficient in syntaxin4 (Stx4 KO EpH4) and EpH4 cells with inducible expression of T7-tagged syntaxin4 (T7–Stx4 EpH4) (Fig. 1C). These cells were then aggregated as previously described (Hirai et al., 1998) and were cultured in reconstituted BM matrix Matrigel, because the myoepithelial cells enveloping luminal epithelial cells *in vivo* actively produce BM components. In conventional hormone-free medium, aggregates of these EpH4 derivatives, which either were deficient in syntaxin4 or inducibly expressed exogenous syntaxin4, did not exhibit any discernible phenotypes (Fig. 1C). In contrast, in the medium containing prolactin, T7–Stx4 EpH4 cell aggregates, regardless of the expression of exogenous syntaxin4, underwent a dramatic cellular arrangement to form multiple lumens inside, somewhat similar to lobular-alveolar development during pregnancy and lactation. Although apicobasal polarity was not clearly established in these cells, such a meaningful cell behavior was not observed in syntaxin4-deficient Stx4 KO EpH4 cells and was more prominent in T7–Stx4 EpH4 cells expressing exogenous syntaxin4 (Fig. 1C). To determine whether syntaxin4 impacts fundamental cell behavior, we compared the shapes of Stx4 KO EpH4 cells to those of parental EpH4 cells in two-dimensional (2D) culture. Treatment with prolactin led to flattened morphology in EpH4 cells, and r-F3, a membrane-impermeable recombinant fragment of syntaxin4 (Glu198–Lys272) that has been shown to act as a potent antagonist of extracellular syntaxin4 (Hirose et al., 2018), substantially attenuated this effect. In contrast, the morphology of Stx4 KO EpH4 cells was unaffected by prolactin and r-F3 treatments, suggesting that the effects of prolactin can be attributed, at least in part, to extracellularly extruded syntaxin4 (Fig. S1). However, we could not test the effect of this antagonistic fragment in 3D culture, since this fragment is rapidly trapped by laminin in Matrigel (Shirai et al., 2017) and would not be accessible to the cells.

Journal of Cell Science (2021) 134, jcs258905. doi:10.1242/jcs.258905

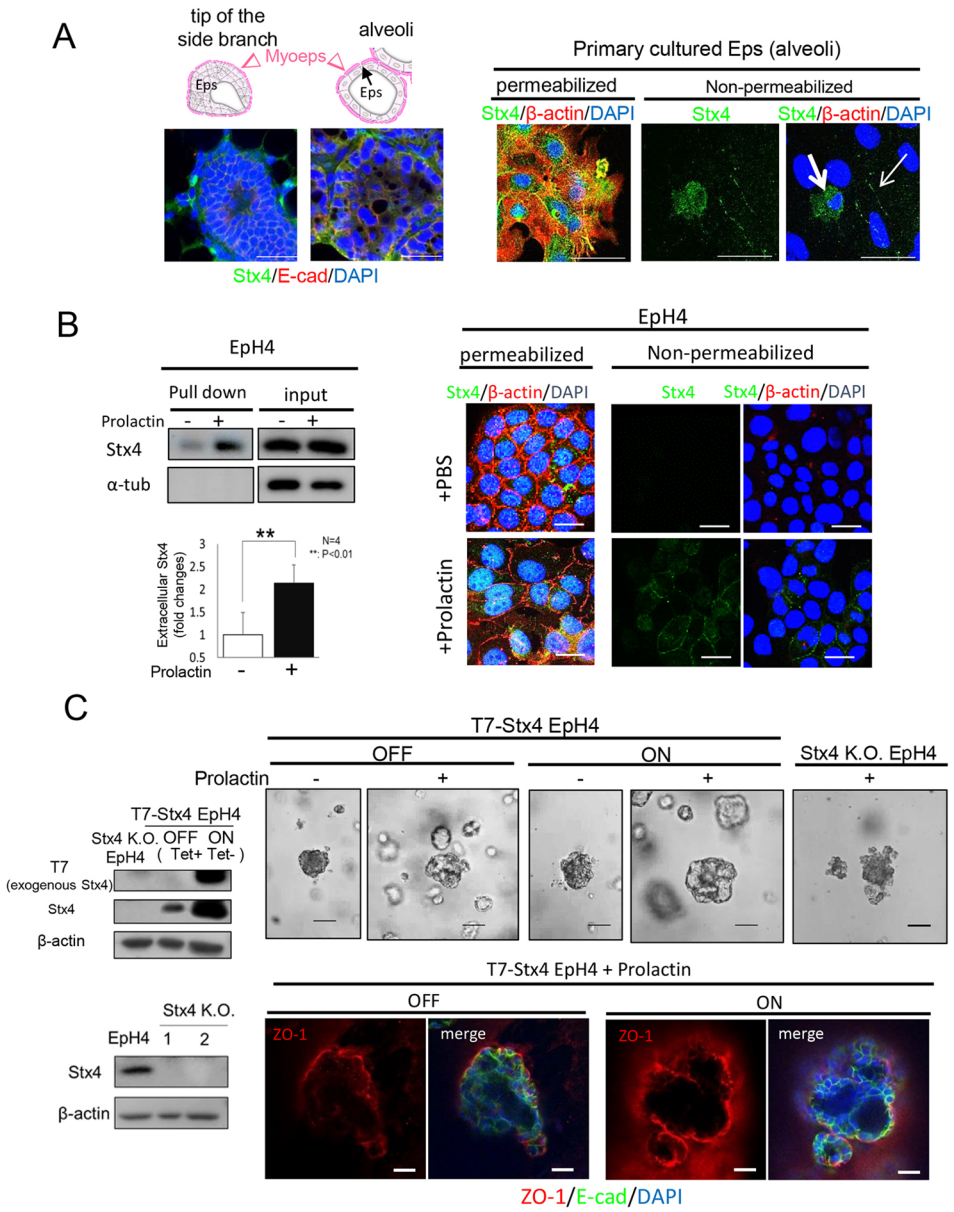

Fig. 1. Effect of syntaxin4 on 3D morphogenesis of mammary gland epithelia. (A) Left upper: schematic diagrams of a tip of side branch (multilayered epithelia) and cystic alveoli in the lobule (single layered epithelial cells). The luminal epithelial cells (Eps, arrow) are surrounded by a layer of myoepithelial cells (Myoeps, arrowhead). Left lower: tip of a side branch or possibly a terminal end bud (left; 7 weeks of age), and alveoli (right; lactation period day 1) in the mouse mammary gland were stained for syntaxin4 (Stx4, green) and E-cadherin (E-cad, red). Nuclei were counterstained with DAPI (blue). Scale bars: 25 µm. Right: mouse mammary Eps were isolated from developing alveoli (13 days of gestation), cultured with prolactin (1 µg/ml) and stained for total (permeabilized) or cell surface (non-permeabilized) β-actin (red) and syntaxin4 (green). Nuclei were counterstained with DAPI (blue). Arrow indicates intercellularly extruded syntaxin4. Bold arrow indicates cell surface syntaxin4. Scale bars: 50 µm. Images are representative of three experiments. (B) EpH4 cells stimulated with prolactin extruded syntaxin4 at the cell surface. Left: biotinylated surface proteins retrieved with NeutrAvidin beads (pull down) from lysate of EpH4 cells (input, 2% of total lysate) were tested for syntaxin4 and cytoplasmic α-tubulin (α-tub). Representative blots are shown, and data are presented as mean±s.d. (*N*=4). ***P*<0.01 (two-tailed, paired Student's *t*-test). Right: EpH4 cells cultured with (+Prolactin) or without (+ PBS) prolactin were stained for total (permeabilized) or cell surface (non-permeabilized) β-actin (red) and syntaxin-4 (green). Nuclei were counterstained with DAPI (blue). Scale bars: 25 µm. Stimulation with prolactin for 24 h led to the translocation of syntaxin4 across the cell membrane in some EpH4 cells. Images are representative of three experiments. (C) Left upper: EpH4 cells with inducible expression of T7-tagged syntaxin4 (T7–Stx4 EpH4) in the presence (Tet+, OFF) or absence (Tet–, ON) of tetracycline and those with complete depletion of syntaxin4 (Stx4 KO EpH4) were assayed for exogenous (T7) and total Stx4. Upon removal of tetracycline, T7–Stx4 EpH4 cells expressed exogenous syntaxin4. Left lower: expression of syntaxin4 in control EpH4 cells and Stx4 KO EpH4 cells generated using different gRNAs (clones 1 and 2). β-actin is shown as a loading control. Blots are representative of three experiments. Right upper: morphology of aggregates of EpH4 derivatives (T7–Stx4 EpH4 cells with Stx4 OFF, T7–Stx4 EpH4 cells with Stx4 ON and Stx4 KO EpH4 cells) cultured in Matrigel with (+) or without (–) prolactin for five days. Scale bars: 50 µm. In response to prolactin, aggregates of the T7–Stx4 EpH4 cells produced multiple lumens, the expansion speed of which roughly depended on the amount of syntaxin4 expressed. By contrast, Stx4 KO EpH4 cells never underwent such a cellular arrangement. As the phenotypic appearance was indistinguishable between clones 1 and 2, only that of clone 2 is shown. Images are representative of three experiments. Right lower: aggregates of T7–Stx4 EpH4 cells cultured in the presence of prolactin in Matrigel were stained for E-cadherin (green) and ZO-1 (red). Nuclei were counterstained with DAPI (blue). Treatment with prolactin induced formation of multiple lumens, regardless of the induction of exogenous syntaxin4; however, clear apicobasal polarity was not established as judged by the localization of ZO-1. Scale bars: 20 µm. Images are representative of six experiments.

Journal of Cell Science (2021) 134, jcs258905. doi:10.1242/jcs.258905

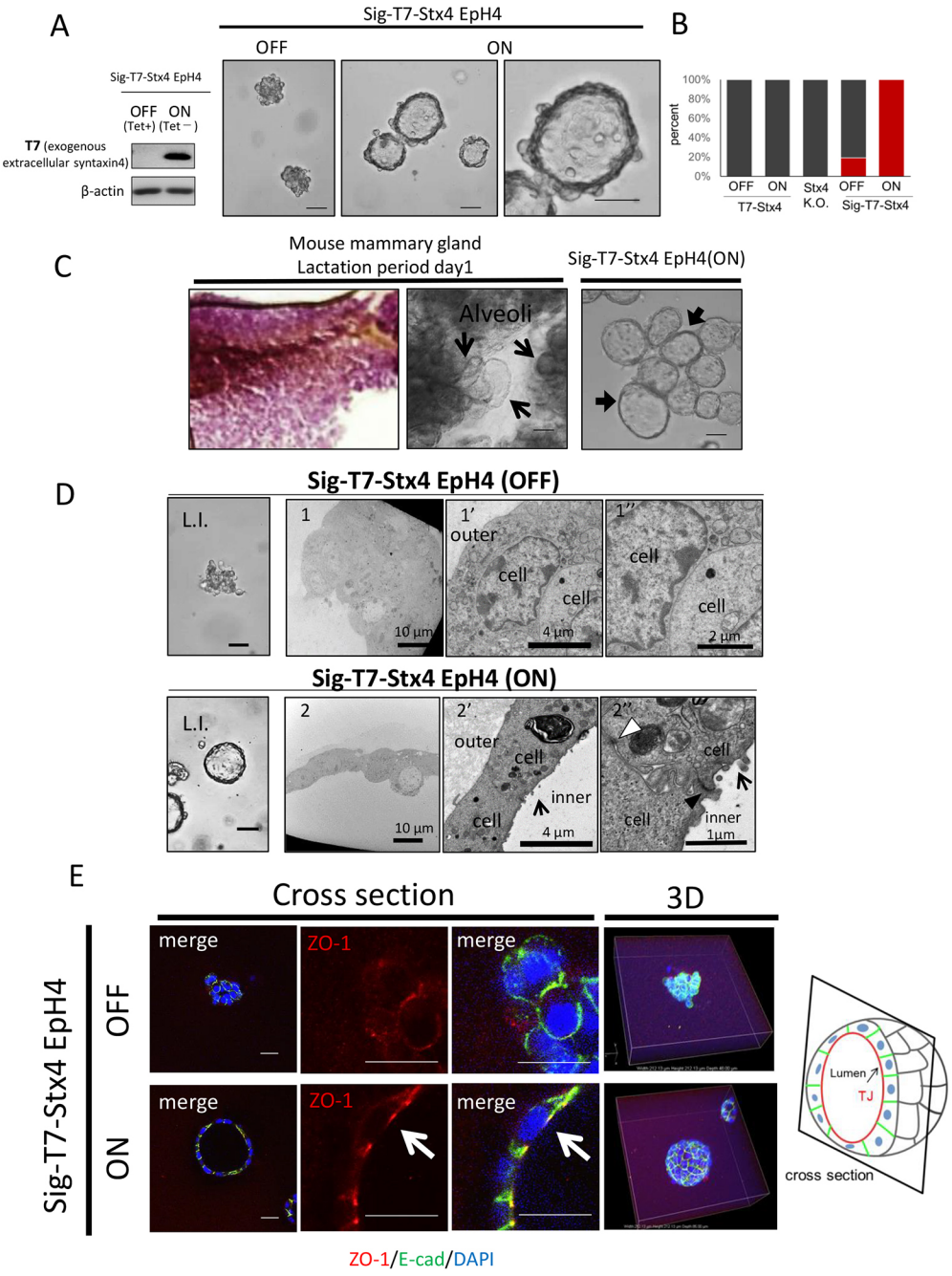

Fig. 2. Analyses of the cystic structures induced by extracellular syntaxin4. (A) Aggregates of EpH4 cells carrying a construct for tetracycline-repressive T7–syntaxin4 containing an N-terminal fusion of a signal peptide (Sig–T7–Stx4 EpH4) were embedded in Matrigel and analyzed for morphological characteristics on day 5 (right). In response to forced expression of extracellular syntaxin4, as assessed by western blotting (left), dramatic cellular arrangements of the cystic structures were induced even in a prolactin-free medium. OFF, Sig–T7–Stx4 expression repressed due to presence of tetracycline (Tet+); ON, Sig–T7–Stx4 expressed in absence of tetracycline (Tet−). The β-actin blot is shown as a loading control. Scale bars: 50 µm. Blots and images are representative of four and ten experiments, respectively. (B) Percentage of cell aggregates with large (more than 30 µm in diameter) central lumen (red) for the indicated EpH4 cell lines and tetracycline conditions (n=20). (C) Left: murine mammary gland at lactation period day 1 stained with Carmine Alum solution. Staining indicates mammary epithelia in the whole gland. Middle: microscopic image of the alveoli (arrows) in the enzymatically dissociated gland is shown. Right: overall structure of the syntaxin4-induced cystic architecture (arrows) of Sig–T7–Stx4 EpH4 aggregates resembles that of alveoli of a lactating gland. Scale bars: 50 µm. Images are representative of six samples. (D) Transmission electron micrographs showing microstructural features of EpH4 cell aggregates with (Stx4 ON; panels 2, 2′ and 2″) or without (Stx4 OFF; panels 1, 1′ and 1″) extracellular expression of Stx4 (Sig–T7–Stx4). Scale bar is indicated in each image. L.I. panels show light micrographs for each category. Scale bars: 50 µm. While the cells without extracellular syntaxin4 remained as tightly packed cell clumps, those with extracellular syntaxin4 formed single-cell-layered cysts possessing developed desmosomes (white arrowhead), polarized TJs (black arrowhead) and microvilli facing toward luminal spaces (arrows). Images are representative of four samples. (E) Left: EpH4 cysts induced by Sig–T7–Stx4 were stained for TJ protein ZO-1 (red) and E-cadherin (green), and are shown in cross-section and as reconstructed 3D images. Nuclei were counterstained with DAPI (blue). ZO-1 was localized at lumen-proximal regions of the cell membrane (arrows) in cells with extracellular syntaxin4 (ON). Cell aggregates without expression of Sig–T7–Stx4 (OFF) are shown for comparison. Scale bars: 20 µm. Right: schematic diagram of the cystic architecture induced by extracellular syntaxin4. Images are representative of four experiments.

Journal of Cell Science (2021) 134, jcs258905. doi:10.1242/jcs.258905

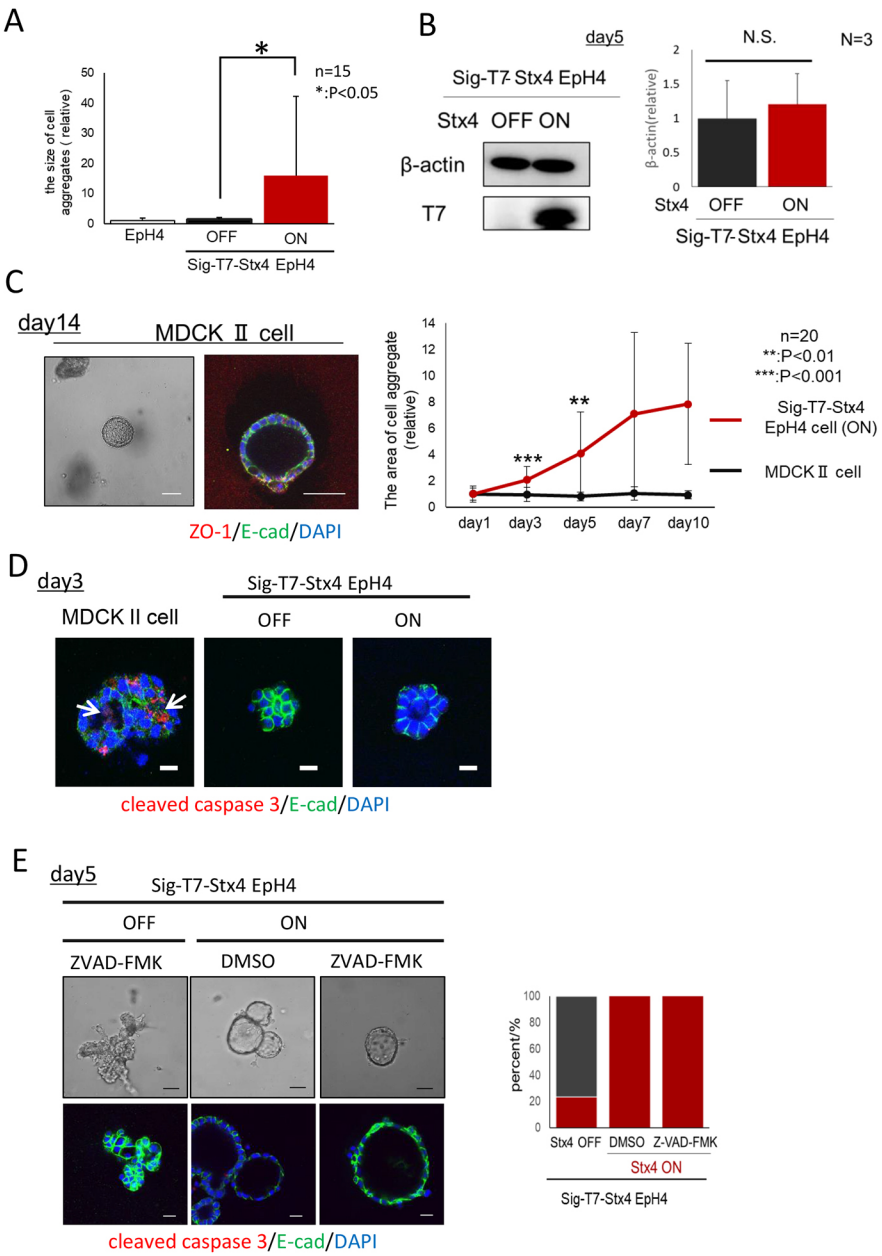

Fig. 3. Comparison of cysts induced in EpH4 cells by syntaxin4 and in MDCK II cells without syntaxin4. (A) Relative size of EpH4 cell aggregates with (ON) and without (OFF) expression of extracellular syntaxin4 (Sig–T7–Stx4) after 5 days of incubation. Data are presented as mean±s.d., *n*=15. (B) The amount of β-actin, a representative of total cell number, was analyzed to determine cellular proliferation in aggregates with (ON) and without (OFF) extracellular syntaxin4 (T7). A representative experiment is shown, and quantitative data are presented as mean±s.d. *N*=3. Extracellular syntaxin4 led to cyst expansion without cell proliferation. (C) Cyst formation in cell aggregates of another epithelial cell line, MDCKII, in Matrigel. Left: microscopic and immunofluorescence images. Green, E-cadherin; red, ZO-1; blue, DAPI. Scale bars: 50 µm. Right: time-dependent size changes in aggregates of Sig–T7–Stx4 EpH4 (Stx4 ON; red) and MDCK II (gray) cells. Data are presented as mean±s.d., *n*=20. While the cyst size of the aggregates of Sig–T7–Stx4 EpH4 cells dramatically increased in a week, that of MDCK II aggregates remained practically unchanged. (D) Aggregates of MDCK II and Sig–T7–Stx4 EpH4 cells were cultured for 3 days and stained for cleaved caspase-3 (red) and E-cadherin (green). Nuclei were counterstained with DAPI (blue). Cleaved caspase-3 was detected in the growing lumen of MDCK II cell aggregates (arrows), but not of Sig–T7–Stx4 EpH4 cell aggregates. Scale bars: 50 µm. Images are representative of four samples. (E) Left: treatment with ZVAD-FMK (20 µM), a pan-caspase inhibitor, for five days did not prevent cyst formation (Stx4 ON condition) in Sig–T7–Stx4 EpH4 aggregates. DMSO, vehicle control. Upper panels, microscopic images. Lower panels, transverse sections stained for E-cadherin (green) and cleaved-caspase3 (red). Nuclei were counterstained with DAPI (blue). Scale bars: 50 µm (upper panel) and 20 µm (lower panel). Right: quantification of the ZVAD-FMK effect on lumen formation induced by extracellular syntaxin4, showing the percentage of aggregates with (red) or without (gray) lumens. Sig–T7–Stx4 EpH4 cells developed palpable lumens, even in the presence of a pan-caspase inhibitor (*n*=20). In A–C, **P*<0.05; ***P*<0.01; ****P*<0.001; N.S., not significant (two-tailed, paired Student's *t*-test).

Induction of clear cystic structure by extracellularly presented syntaxin4

To clarify the effect of extracellular syntaxin4, we generated EpH4 cells with inducible expression of T7-tagged syntaxin4 fused with a signal peptide for extracellular translocation (Sig–T7–Stx4). Upon induction of syntaxin4 on the surface of all cells, Sig–T7–Stx4 cell aggregates underwent dramatic cellular arrangement to form cystic structures with a large central lumen, even in the absence of prolactin (Fig. 2A,B). Although the cellular arrangement was so dramatic that the additive effects of prolactin on these cells were not appreciable, the phenotypic appearance (exhibiting either multiple lumens or single lumen) was clearly dependent upon the mode of extracellular expression (either by a subset of cells or by all cells in an aggregate) of syntaxin4 (Figs 1C and 2A; Fig. S2). These results highlight the effect of extracellularly extruded syntaxin4 on epithelial morphogenesis in the mammary gland. The overall cystic structure of Sig–T7–Stx4 cells in Matrigel was similar to that of the alveoli in lactating mammary glands (Fig. 2C). Transmission electron microscopy analyses revealed that these cysts were composed of single-layered epithelial sheets with representative intercellular junctional complexes, including desmosomes and tight junctions (TJs) (Fig. 2D,E). In addition, the well-developed microvilli of cells in the cystic structure were exposed only toward the luminal spaces, with an accumulation of a TJ component, zonula occludens-1 (ZO-1, also known as TJP1), at the lumen-proximal region, suggesting that these cells acquired apicobasal polarity (Fig. 2D,E). According to the 3D images, the basal surface of the cysts appeared smooth (Fig. 2E). In contrast, in the absence of induction of extracellular syntaxin4, these cells were alive but remained in tightly packed cell clumps (Fig. 2D,E). These results demonstrate that extracellularly presented syntaxin4 contributes to the reorganization of cell aggregates into cystic structures with apicobasal polarity in Matrigel, which is reminiscent of the epithelial compartment in the mammary alveoli.

Journal of Cell Science (2021) 134, jcs258905. doi:10.1242/jcs.258905

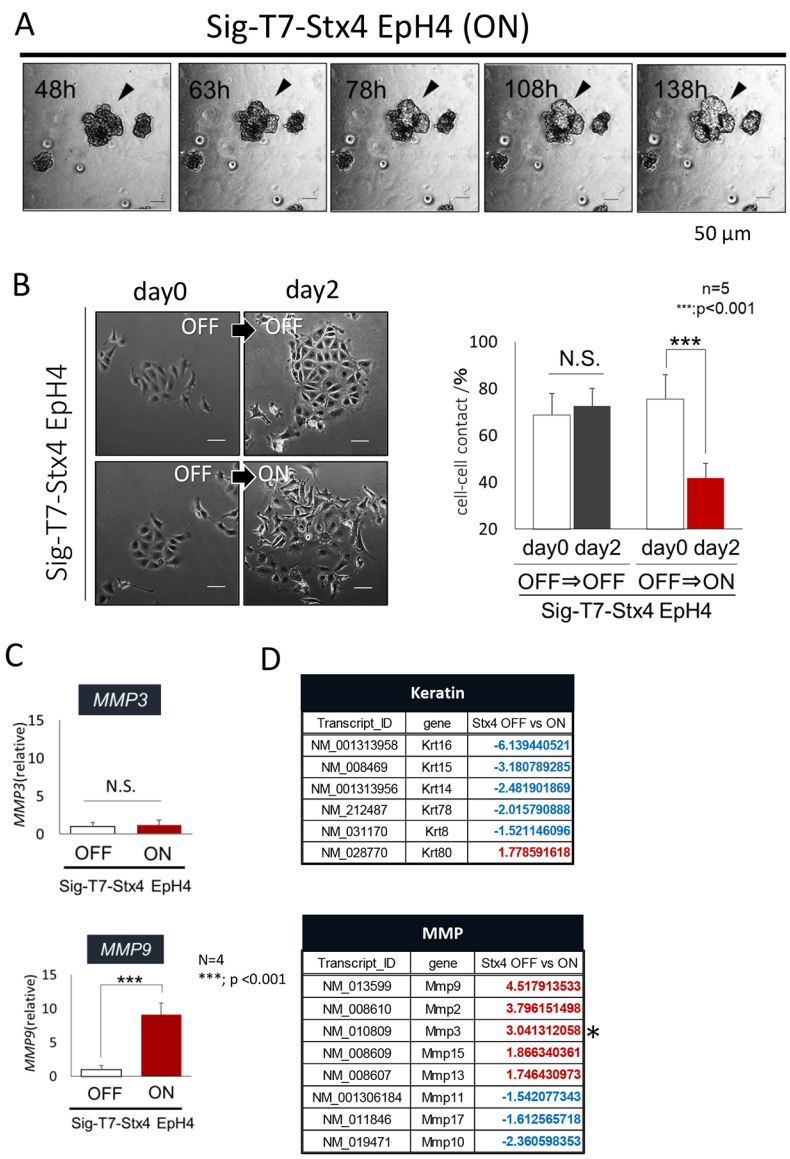

Fig. 4. Behaviors of individual EpH4 cells in response to extracellular syntaxin4. (A) Time-lapse images of aggregates of Sig–T7–Stx4 EpH4 cells expressing extracellular syntaxin4 (ON) in Matrigel. After 48 h of induction, the onset of cellular arrangement towards the formation of the cystic structure became apparent. Subsequently, the overall size of the cell aggregates gradually increased as the inner portion became transparent. Arrowheads, cell aggregates producing a large central lumen. Scale bars: 50 µm. Images are representative of eight samples. (B) Left: micrographs of Sig–T7–Stx4 EpH4 cells cultured on dishes with (ON) or without (OFF) induction of extracellular syntaxin4 for two days. Scale bars: 50 µm. Right: percentage of the cells exhibiting direct cell–cell contact in each condition. The number of cells adhering to each other was counted on days 0 and 2. Data are presented as mean±s.d. *n*=5. Extracellular syntaxin4 disrupted intercellular adhesion and elicited migratory responses. (C) mRNA expression, as assessed using qRT-PCR, of *Mmp3* and *Mmp9* in EpH4 cells with (ON) or without (OFF) extracellular syntaxin4. Data are presented as mean±s.d. *N*=4. (D) RNA sequencing analyses revealed the induction of the onset of EMT-like cell behaviors by extracellular syntaxin4. Among the comprehensive data sets, all genes showing more than 1.5-fold change in expression of 'keratin' (11 keratins in total) or 'MMP' (13 MMPs in total) that are assigned to the cell migration category in the Gene Ontology terms were extracted and listed. The fold change in expression for genes that were upregulated and downregulated in response to extracellular syntaxin4 are shown in red and blue, respectively (asterisk indicates *Mmp3*; although *Mmp3* is listed as one of the upregulated genes, the qRT-PCR analysis shown in C did not detect this change). ***P<0.001; N.S., not significant (two-tailed, paired Student's *t*-test).

Syntaxin4-induced morphogenesis is independent of cell growth and apoptosis

Although the size of syntaxin4-induced cysts continued to increase for several days, there were no significant differences in the total number of cells, regardless of induction by extracellular syntaxin4, as judged by the amount of β-actin (Fig. 3A,B). This was not the case when the same experiments were performed using another epithelial cell line, MDCK II, which reportedly exhibits clear polarity and possesses the ability to form cystic structures in Matrigel, even in the absence of hormonal stimuli and exogenous transgenes. While the sizes of MDCK II cell aggregates were practically unchanged during culture, each formed a luminal space within a few days (Fig. 3C). Given that the production of lumen in MDCK II cells involves apoptotic elimination of Matrigel-free central cells in the aggregates (Martín-Belmonte et al., 2008), those formed by aggregates of EpH4 cells in the presence of extracellular syntaxin4 might be independent of apoptotic cell death. As expected, the active form of effector caspase (caspase 3) was detectable in the luminal side of MDCKII cysts, but not in the syntaxin4-induced ones (Fig. 3D), and the formation and expansion of the latter were not hindered by the functional ablation of caspases with the inhibitor ZVAD-FMK (Fig. 3E).

EpH4 cells improve locomotive ability in response to extracellular syntaxin4

Next, we addressed successive cellular migratory behaviors in the aggregates in response to extracellular syntaxin4. Time-lapse imaging revealed that the inner cells in the aggregates do not succumb to apoptosis but actively migrate (Fig. 4A; Movie 1). In 2D cultures, these cells with morphological changes dissociated from colonies and migrated outward upon induction of extracellular syntaxin4 (Fig. 4B), implying an onset of EMT. Among all keratin genes tested (11 keratins in total), six keratins exhibited significant changes in their expression (more than 1.5-fold change) in response to extracellular syntaxin4, with five of these appearing to be downregulated. In addition, eight of 13 genes encoding matrix metalloproteinases (MMPs) showed significant changes, and the three genes with the largest changes, which included *MMP9*, appeared to be clearly upregulated (Fig. 4C,D).

Behaviors of Matrigel-attached EpH4 cells expressing extracellular syntaxin4

The cell behaviors observed were quite different when cells were directly attached to Matrigel; changes in mobility and intercellular

Journal of Cell Science (2021) 134, jcs258905. doi:10.1242/jcs.258905

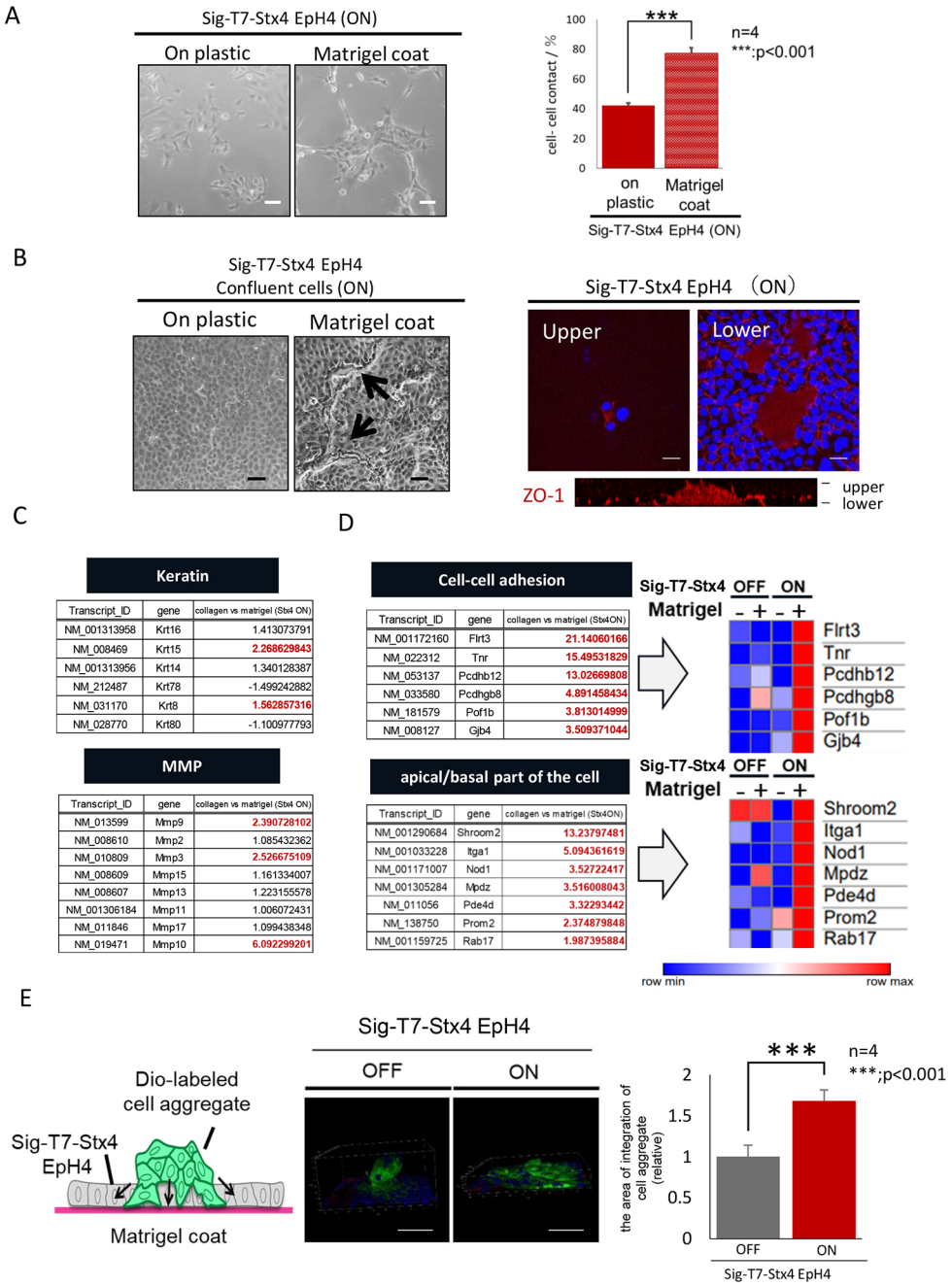

Fig. 5. See next page for legend.

adhesiveness in response to extracellular syntxin4 were visibly attenuated in the 2D culture (Fig. 5A). In addition, confluent cell sheets on Matrigel displaying sustained expression of extracellular syntaxin4 often formed dome-like structures with clear intercellular junctions (Fig. 5B). We have previously shown that the C-terminal globular domain of laminin, a major BM component, and glycosaminoglycan (GAG) side chains of a laminin receptor interact with extracellular syntaxin4 so as to potentially counteract its function (Shirai et al., 2017). However, RNA sequencing analyses revealed that changes in the expression of EMT markers affected by extracellular syntaxin4 (Fig. 4C,D) were not restored in cells stimulated simultaneously with Matrigel. Although some keratin genes were prone to reactivation, the augmented expression of the MMPs remained constant or was further upregulated (Fig. 5C). In addition, expression of several molecular elements involved in intercellular adhesions or epithelial polarity were dramatically upregulated in response to simultaneous stimulation with both extracellular syntaxin4 and Matrigel (Fig. 5D), suggesting that extracellular syntaxin4 and BM components do not simply antagonize each other or propagate individual signals independently, but cooperatively elicit unique responses in the epithelial cells (Fig. 5C,D). Furthermore, we also found that EpH4 cells situated away from Matrigel could smoothly integrate into the confluent cell sheet on Matrigel if they expressed extracellular syntaxin4 (Fig. 5E). Such syntaxin4-triggered distinct regulatory effects depending on the influence of Matrigel might account for the

Fig. 5. Distinct behaviors in syntaxin4-expressing EpH4 cells in contact with Matrigel. (A) Left: micrographs of growing Sig–T7–Stx4 EpH4 cells expressing extracellular syntaxin4 (ON) on dishes coated with and without Matrigel. Scale bars: 20 µm. Right: percentage of cells exhibiting direct cell–cell contacts on day 2. The reduction of intercellular adhesion induced by extracellular syntaxin4 was apparently recovered if cells directly adhered to Matrigel. Data are presented as mean±s.d. *n*=4. (B) Confluent Sig–T7–Stx4 EpH4 cells expressing extracellular syntaxin4 (ON) on dishes coated with and without Matrigel. Left: representative micrographs. Right: cells in the upper and lower planes were stained for ZO-1 (red) and DAPI (blue). The *z*-stack image for ZO-1 is presented below. Scale bars: 50 µm. The cells on Matrigel with extracellular syntaxin4 retained the intercellular adhesion and often formed enclosed dome-like structures (arrows). Images are representative of six samples. (C) RNA-sequencing analyses of Sig–T7–Stx4 EpH4 cells expressing extracellular syntaxin4 (Stx4 ON) cultured on Matrigel versus on collagen. With regard to all keratin and MMP genes showing more than 1.5-fold expression change in response to extracellular syntaxin4 (Fig. 4D), expression of only *Krt15* and *Krt8* was restored, but expression of *Mmp9*, *Mmp3* and *Mmp10* was further facilitated by culturing on Matrigel. Genes showing significant upregulation (more than 1.5-fold) are colored red. (D) Left: genes showing significant changes in expression (more than 1.5-fold) in the RNA-sequencing analysis described in C that are also assigned to the Gene Ontology category 'cell–cell adhesion' (the six genes with greatest increase in expression in the Matrigel sample are shown in descending order, from 65 genes in total) or 'apical/basal part of the cell' (the seven genes with greatest increase in expression in the Matrigel sample are shown in descending order, from 31 genes in total) appeared to be upregulated when cells with extracellular syntaxin4 were affected simultaneously by Matrigel. Right: heatmap analysis of the expression of these genes in the indicated experimental conditions demonstrates synergistic effects of extracellular syntaxin4 and Matrigel on the acquisition of unique epithelial characteristics. (E) Left: diagram of aggregate integration on Matrigel. Middle: reconstructed 3D images of the integration of cell aggregates into a single cell layer on Matrigel. The floating aggregates of Sig–T7–Stx4 EpH4 cells pre-labeled with a lipophilic green fluorescent dye (DiO) were seeded onto a confluent cell sheet on Matrigel, followed by five days of incubation with (ON) or without (OFF) induction of extracellular syntaxin4. Red, E-cadherin; blue, DAPI. Scale bars: 50 µm. Right: relative area of DiO-labeled cells integrated into Matrigel-bound cell sheets. Data are presented as mean±s.d. *n*=4. The cell aggregates free from Matrigel smoothly integrated into the Matrigel-adherent confluent cell sheet if they expressed extracellular syntaxin4. ***P<0.001 (two-tailed, paired Student's *t*-test).

multicellular arrangement, that is, in response to extracellular syntaxin4, cells that are less affected by BM actively move to and smoothly integrate into the polarized cell layer facing the BM, and this layer acquires unique epithelial characteristics to undergo dramatic cellular arrangements for the formation and expansion of cystic structures. Consistent with this, when cell aggregates were embedded in collagen gel, the outermost cell population was radially scattered instead of contributing to luminal morphogenesis (Fig. S3).

Extracellular syntaxin4 triggers turnover of E-cadherin

We next addressed the effect of syntaxin4-dependent dysregulation on cell–cell adhesion systems in the absence of the BM effect. Previously, we have shown that extracellular syntaxin4 directly binds to E-cadherin, a critical player in epithelial cell–cell adhesion (Hirose et al., 2018), to hinder its intrinsic cell adhesive function without affecting its mRNA expression. The direct association between the central and membrane-proximal domains of syntaxin4 and E-cadherin extracted from EpH4 cells was ascertained again (Fig. S4). We observed a significant reduction in the intact form of syntaxin4 in cells after treatment with prolactin, which was partly prevented by addition of chloroquine (an inhibitor of the protein-elimination system in lysosomes) in a dose-dependent manner (Fig. 6A,B). Intriguingly, extracellular expression followed by lysosomal degradation of extracellular syntaxin4 appeared to be coincident with the appearance and lysosomal degradation of a 90 kDa form of E-cadherin protein (Fig. 6B). To further clarify whether the extracellular but not the intracellular form of syntaxin4 is responsible for these phenomena, we compared the effects of intact syntaxin4 and its signal peptide-connected form in the absence of prolactin but in the presence of chloroquine. We found that the dose-dependent effects of chloroquine treatment were reproduced only for the extracellular form of syntaxin4, demonstrating that extracellularly present syntaxin4 readily undergoes lysosomal degradation along with the 90 kDa E-cadherin (Fig. 6C,D). Based on the assumption that a direct interaction between syntaxin4 and E-cadherin at the cell surface initiates the elimination process, we analyzed the expression pattern and physical characteristics of these proteins in cells treated with chloroquine. A subpopulation of syntaxin4 and E-cadherin co-assembled to converge on the same dot-like structures in the cytoplasm, although their original expression was at the cell surface, exhibiting insoluble characteristics (Fig. 6E,F; Fig. S5A). Regarding the 90 kDa form of truncated E-cadherin, polyclonal antibodies against cytoplasmic domains of E-cadherin failed to recognize this form (Fig. S5B), and its abundance was clearly decreased by treatment with the proteasome inhibitor lactacystin (Fig. 6G), suggesting that the shift in the molecular mass of E-cadherin (from 124 kDa to 90 kDa) can be ascribed to the proteasomal processing of its cytoplasmic tail. However, despite the fact that E-cadherin was processed, internalized and degraded in cells with extracellular syntaxin4, the amount of the functional 124 kDa form was unaltered (Fig. 6D). Taken together with the observation that mRNA expression of E-cadherin was not affected by extracellular syntaxin4 in this cell system (Fig. S5C), these results suggest a dramatic increase in E-cadherin turnover with intermittent exposure of 'tailless' E-cadherin in cells with extracellular syntaxin4. Interestingly, the syntaxin4-induced turnover of E-cadherin remained in cells that were in contact with Matrigel (Fig. S5D), confirming that signals by extracellular syntaxin4 and BM components do not simply antagonize each other.

Syntaxin4-dependent E-cadherin turnover and the role of Matrigel in a simple cell system

To further define the biological significance of the effect of extracellular syntaxin4 on E-cadherin turnover, the subsequent intermittent exposure of tailless E-cadherin, and the concerted action with BM components, we conducted experiments using fibroblastic L cells, which have no intrinsic cell adhesion molecules and are much less responsive to BM components (Kiener et al., 2009; Nagafuchi et al., 1987). L cells with stable expression of the full-length E-cadherin transgene (designated as EL cells) exhibit cell-adhesive properties caused solely by E-cadherin (Nagafuchi et al., 1987). Notably, however, expression of the E-cadherin transgene alone is sufficient to induce strong cell-adhesive properties in L cells (Nagafuchi et al., 1994), and EL cells do not lose features of fibroblasts (Chen and Obrink, 1991), suggesting that L cells endogenously possess or can rapidly form catenin–actin complexes for the cytoskeletal linkage of E-cadherins. We found that EL cells additionally expressing the 'tailless' form of E-cadherin appeared to retain cell–cell adhesion in 2D, but this gradually weakened the E-cadherin-mediated cell–cell adhesion without affecting the amount of functional full-length E-cadherin (Fig. S6). Based on these observations, we generated EL cells with inducible expression of extracellular syntaxin4 and used them for biological validation. Upon induction of extracellular syntaxin4, the abundance and insolubility of syntaxin4 and the 90 kDa form of E-cadherin appeared to increase in the presence of chloroquine,

Journal of Cell Science (2021) 134, jcs258905. doi:10.1242/jcs.258905

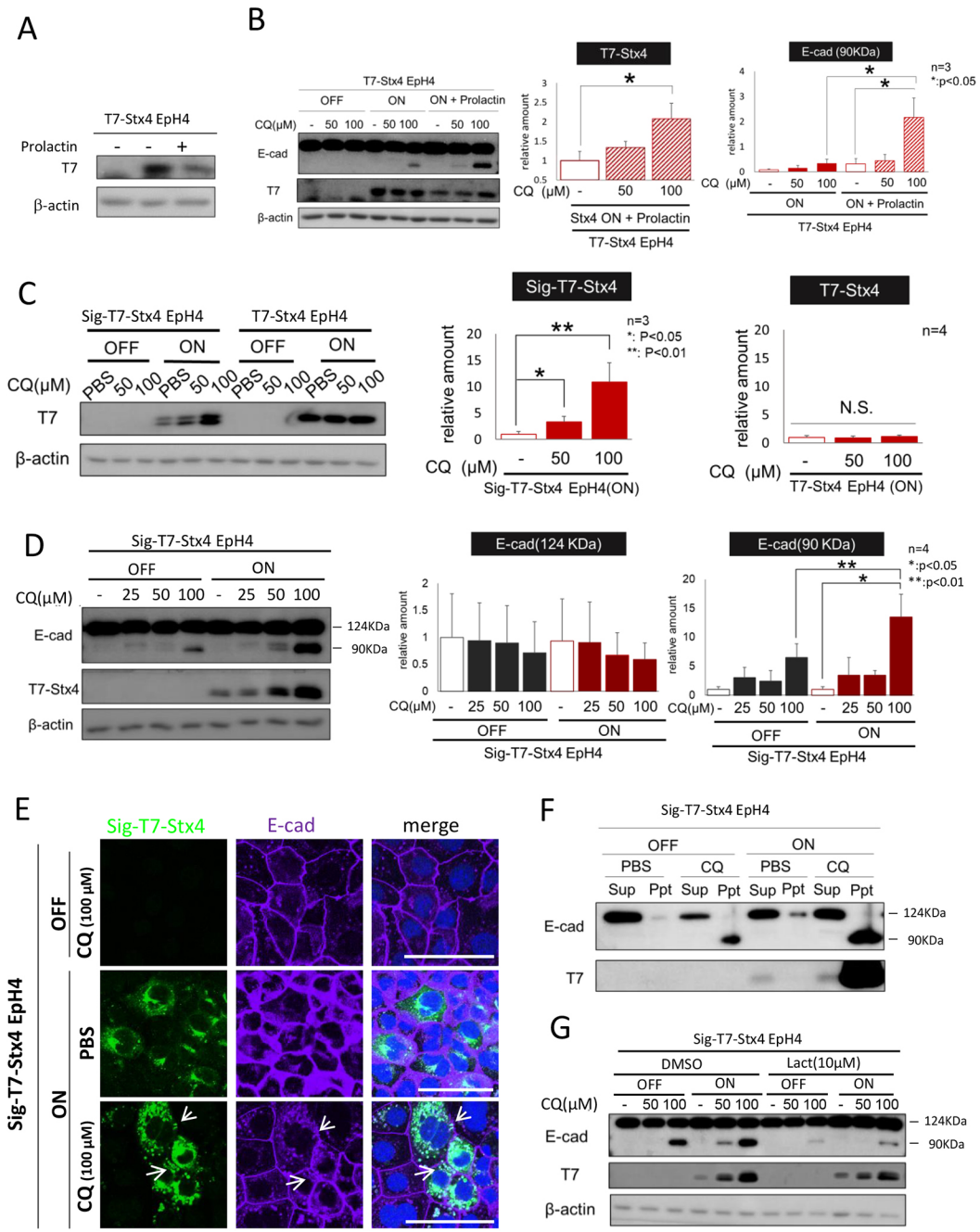

Fig. 6. See next page for legend.

indicating that the acceleration in E-cadherin turnover also occurs in this cell system (Fig. 7A,B). Although the instantaneous activity of E-cadherin was practically unchanged by the extracellular expression of syntaxin4 (Fig. S7), cells in syntaxin4-expressing EL cell aggregates gradually weakened cell–cell contacts in 3D culture, and the outermost cells became scattered with exposed filopodial protrusions (Fig. 7C), confirming the extracellular role of syntaxin4 as a functional repressor of E-cadherin.

This study demonstrates a novel and plausible mechanism underlying dynamic cellular arrangements for epithelial morphogenesis that could explain how mammary epithelial cells build the alveolar structure during pregnancy. Hormones actively secreted during the gestational period trigger temporal translocation of syntaxin4 across the membrane, and extracellularly extruded syntaxin4 exerts distinct morphogenic functions depending on the cellular context, modulated by BM signals. In cell populations that are less affected by BM-producing myoepithelial cells, extracellular syntaxin4 causes cells to migrate and integrate into the cell layer facing the BM and myoepithelial cells, whereas in the cell population that is in contact with the BM and myoepithelial cells, extracellular syntaxin4 propagates unique signals for the construction of cystic structures (Fig. 8).

DISCUSSION

Membrane translocation of syntaxin4

We first demonstrated that the lactogenic hormone prolactin induces membrane translocation of the t-SNARE protein syntaxin4 in EpH4 cells, as observed in cultured lactogenic mammary epithelial cells.

Fig. 6. Effect of extracellularly extruded syntaxin4 on E-cadherin expression. (A) The amount of exogenous syntaxin4 (without the signal peptide; T7) in T7–Stx4-expressing EpH4 cells was decreased by prolactin, which provoked extracellular translocation of syntaxin4. β-actin was used as an internal control. A representative example of three experiments is shown. (B) Left: the decrease in syntaxin4 shown in A was ascribed to lysosomal degradation, as judged by treatment with chloroquine (CQ), a potent inhibitor of lysosomal degradation. Treatment with prolactin in addition to CQ increased abundance of the 90 kDa form of E-cadherin (Ecad, lower band), which is readily degraded in lysosomes. OFF, expression of T7-tagged Stx4 repressed; ON, expression of T7-tagged Stx4 induced. Right: quantification of the effects of CQ. Data are presented as mean±s.d. *n*=3. (C) Left: extracellularly expressed syntaxin4 (Sig–T7–Stx4), but not the intact form of syntaxin4 (T7–Stx4), was actively degraded in lysosomes, even in the absence of prolactin. Western blots show exogenous Stx4 (T7) in the indicated cell lines treated with CQ or with PBS as a control. β-actin was used as an internal control. Right: CQ-dependent changes in the amount of extracellular (Sig–T7–Stx4, *n*=3) and intact (T7–Stx4, *n*=4) forms of exogenous syntaxin4. Data are presented as mean±s.d. (D) E-cadherin (E-cad) expression in Sig–T7–Stx4 cells treated with CQ for 12 h. Left: the amount of cleaved E-cadherin (90 kDa), which is readily degraded in lysosomes, was significantly higher in cells with extracellular syntaxin4. β-actin was used as an internal control. Right: CQ-dependent changes in the amount of intact (124 kDa) and cleaved (90 kDa) forms of E-cadherin. Data are presented as mean±s.d. *n*=4. (E) CQ-treated Sig–T7–Stx4 EpH4 cells with (ON) or without (OFF) induction of Sig–T7–Stx4 expression were stained for E-cadherin (E-cad, magenta) and syntaxin4 (T7, green). Nuclei were counterstained with DAPI. In the presence of CQ, E-cadherin and syntaxin4 were colocalized in the cytoplasm (arrows). Scale bars: 20 µm. Images are representative of three experiments. (F) Sig–T7–Stx4 EpH4 cells with or without induction of Sig–T7–Stx4 expression that were cultured with or without CQ (CQ or PBS alone, respectively) were treated with a lysis buffer, and the soluble (Sup) and insoluble (Ppt) fractions were tested for E-cadherin and extracellular syntaxin4 (T7). Both cleaved E-cadherin (90 kDa) and extracellular syntaxin4 were detectable almost exclusively in the insoluble fraction. (G) Treatment of Sig–T7–Stx4 EpH4 cells with a proteasome inhibitor, lactacystin (Lact; 10 µM), dramatically reduced the appearance of 90 kDa E-cadherin. DMSO, vehicle control. β-actin was used as an internal control. Data in F and G are representative of three experiments. **P*<0.05; ***P*<0.01 (two-tailed, paired Student's *t*-test).

While this could be a key event for the subsequent cellular arrangement, the machinery for extracellular extrusion of syntaxin4 is completely unknown to date. However, extrusion of epimorphin, a cognate membrane-tethered syntaxin, may provide referential information, such as the involvement of Ca^{2+} influx, which leads to extracellular extrusion of a multi-protein complex containing epimorphin and phosphatidylserine-bound annexin II (ANXA2) from cells (Hirai et al., 2007). Prolactin has been reported to consistently increase Ca^{2+} uptake in the cytoplasm (Bolander, 1985), and annexin II is involved in prolactin-induced milk secretion (Burgoyne et al., 1991; Zhang et al., 2018). Alternatively, stimulated mammary epithelial cells that are capable of secreting intracytoplasmic lipids containing phosphatidylserine (Smoczyński, 2017) are thought to export syntaxin4 extracellularly together with milk fat globules.

Extracellular syntaxin4 increases cellular motility and accelerates E-cadherin turnover

Once presented extracellularly, syntaxin4 cooperated with BM components to trigger a dramatic arrangement in cells. While a previous study suggested the possible contribution of apoptosis to mammary luminal morphogenesis (Debnath et al., 2002), a recent report has demonstrated that this process could proceed without the requirement of cell demise (Akhtar and Streuli, 2013; Neumann et al., 2018). In line with these observations, we demonstrated that syntaxin4-induced mammary cyst formation proceeds solely by spatiotemporal changes in epithelial cell adhesion, mobility and polarity. Notably, extracellularly exposed syntaxin4 elicited the onset of EMT-like cell responses if the cells were free from the effects of BM. This raises the question as to how syntaxin4 confers locomotive ability in these cells. To this end, we showed that syntaxin4 extruded extracellularly became accessible and directly bound to the major intercellular adhesion molecule E-cadherin via its central and membrane-proximal domains, which could be a cue for the degradation of E-cadherin. Experiments using inhibitors of protein elimination systems showed that the cytoplasmic domain of E-cadherin is degraded by the proteasome upon being associated with syntaxin4 in the extracellular environment, which gives rise to the production of a 90 kDa form that lacks a cytoplasmic tail for cytoskeletal linkage. The protein complex containing the 'tailless' form of E-cadherin and syntaxin4 was then rapidly internalized, delivered to lysosomes and displayed highly insoluble characteristics, after which it was ultimately eliminated. Dysfunctional E-cadherin is known to be ubiquitylated in the juxtamembrane domain and degraded by the proteasome and subsequently by lysosomes (Sako-Kubota et al., 2014). In addition, internalization of E-cadherin in EpH4 cells upon EMT has been shown to be mediated by clathrin-coated vesicles, which are retrievable only from the highly insoluble fraction (Janda et al., 2006). Given that E-cadherin homeostasis is regulated by the small GTPase Cdc42, which is indispensable for alveolar development in mammary glands (Druso et al., 2016; Georgiou et al., 2008; Leibfried et al., 2008), elucidation of its relationship with extracellular syntaxin4 is an important issue that needs to be addressed in future research. While the rapid elimination of 'tailless' E-cadherin and unaltered E-cadherin mRNA expression was obvious in cells with syntaxin4, the amount of functional full-length E-cadherin appeared to be constantly maintained, implying that translation of this adhesion molecule is augmented by syntaxin4. Although further experiments using syntaxin4-transfected cells and translation inhibitors were not feasible because the expression of the syntaxin4-transgene would also be repressed, we have shown previously that the abundance E-cadherin protein, but not mRNA, is dramatically decreased in response to extracellular syntaxin4 in some other cell types (Hagiwara-Chatani et al., 2017; Hagiwara et al., 2013), indicating that E-cadherin translation is facilitated only in certain cell types. Nevertheless, the constant expression and active elimination of E-cadherin suggests active turnover and intermittent disruption of the E-cadherin-mediated intercellular adhesion system.

Cooperation between extracellular syntaxin4 and BM components

E-cadherin, as a major intercellular adhesion molecule, is linked to the cytoskeleton, and its turnover has been shown to severely affect the collective migration of epithelia (Brüser and Bogdan, 2017; Kota et al., 2019; Kowalczyk and Nanes, 2012; Song et al., 2013; Takeichi, 2014). Temporal reduction in epithelial identity, including loss of polarity and increased cell motility, has been reported in inner cell populations of stratified epithelia during active morphogenesis (Ewald et al., 2012). In contrast, E-cadherin dynamics are not the sole determinant of locomotive behavior in these cells. We observed that the effect of forced expression of 'tailless' E-cadherin was relatively weak in EL cells compared to the effect in EpH4 cells; both cell types similarly expressed functional full-length E-cadherin, but changes in the cellular context (expression of EMT-related markers, for example) were more prominent in EpH4 cells (data not shown). In addition, although

Journal of Cell Science (2021) 134, jcs258905. doi:10.1242/jcs.258905

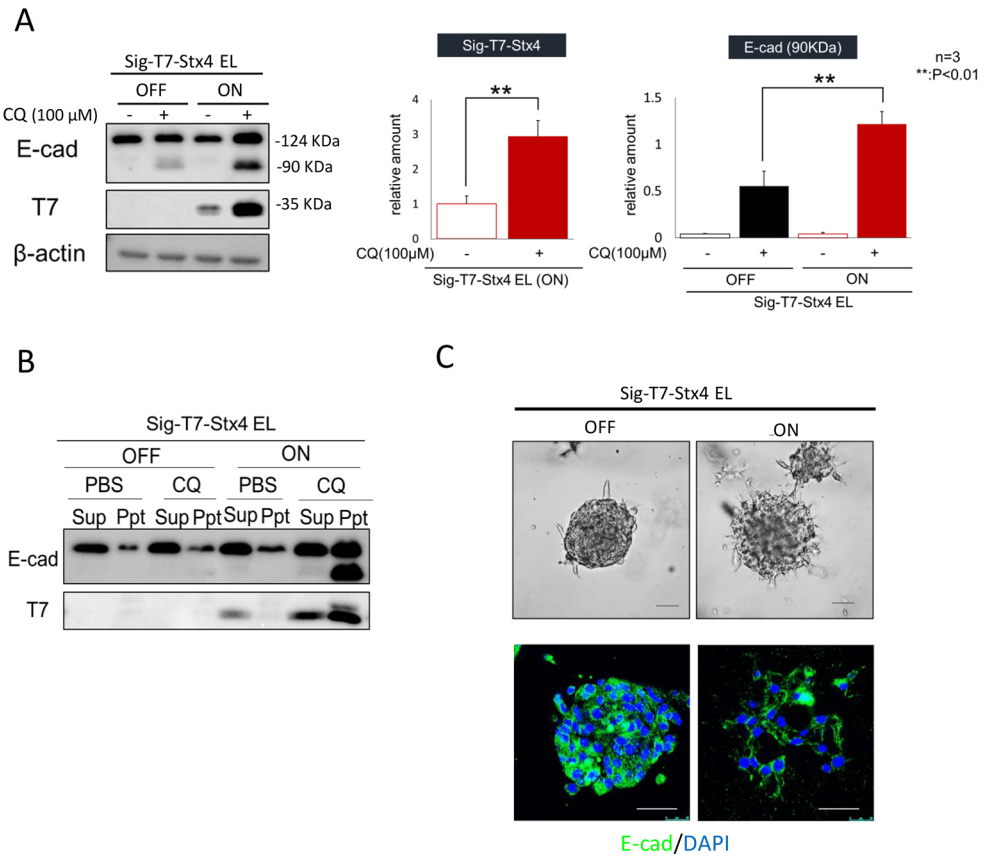

Fig. 7. Validation of the functional coordination model involving syntaxin4 and laminin. (A) Left: L cells expressing exogenous E-cadherin (EL cells), which display intercellular adhesive properties only with E-cadherin (E-cad), were stably transfected with the tetracycline-regulatable Sig–T7–Stx4 construct (Sig–T7–Stx4 EL; OFF, repression of Sig–T7–Stx4 expression; ON, induction of Sig–T7–Stx4 expression) and cultured in the presence or absence of chloroquine (CQ; 100 μM). EL cells readily produced the degraded form of E-cadherin (90 kDa) when they expressed extracellular syntaxin4 (T7). β-actin was used as an internal control. Right: quantification of exogenous extracellular syntaxin4 and 90 kDa E-cadherin. Data are presented as mean±s.d. *N*=3. ***P*<0.01 (two-tailed, paired Student's *t*-test). (B) Expression of extracellular syntaxin4 conferred the characteristic feature of insolubility upon E-cadherin expression. In response to exogenous extracellular syntaxin4 (ON), EL cells produced 90 kDa E-cadherin, which was detectable in the insoluble (Ppt), but not in the soluble (Sup) fraction with extracellular syntaxin4. Cells were cultured either with CQ (0.1 mM) or with PBS as a control, as indicated. A representative of three experiments is shown. (C) Aggregates of Sig–T7–Stx4-EL cells were cultured for 7 days in Matrigel. Upper panels: representative light micrographs. Lower panels: aggregates immunostained for E-cadherin (green), and nuclei were counterstained using DAPI (blue). EL cells, which adhere each other solely by E-cadherin and are much less responsive to BM signals than EpH4 cells, gradually disseminated and scattered in Matrigel in response to the extracellular expression of syntaxin4. Scale bars: 25 μm. Images are representative of three experiments.

active turnover of E-cadherin also occurred in syntaxin4-expressing EpH4 cells adhering to reconstituted BM Matrigel, EMT-like cell behaviors were not observed even in the presence of extracellular syntaxin4. Instead, these cells were tightly connected to each other, with a well-developed intercellular junctional apparatus, and displayed apicobasal polarity. Furthermore, cells cultured on Matrigel often formed enclosed, single-layered, dome-like structures when they expressed extracellular syntaxin4. RNA sequencing analyses revealed that these cells acquired unique epithelial characteristics for the formation of enclosed and well-polarized cysts. Conversely, cell populations that were less affected by BM might actively migrate in response to extracellular syntaxin4 and smoothly integrate into cell layers facing the BM, thus participating in the production of cystic structures. This model of functional coordination involving both prolactin-induced extracellular syntaxin4 and BM components clearly rationalizes the spatial cellular dynamics and plasticity observed in prolactin-triggered luminal morphogenesis in mammary epithelia *in vivo*. We consistently detected a significant difference in the locomotive behaviors of the same cells with extracellular syntaxin4 in collagen gels, and of syntaxin4-expressing EL cells that were less responsive to laminin. The outermost cell populations in both cases dissociated and radially scattered in the 3D substrates.

Extracellular extrusion of syntaxins and the possible role of plasmalemmal syntaxins

We have previously shown that extracellularly extruded epimorphin exerts a function similar to that of syntaxin4 in terms of induction of luminal morphogenesis (Bascom et al., 2005; Hirai, 2001; Hirai et al., 1992; Lehnert et al., 2001). Whereas epimorphin is produced in mammary myoepithelial cells and secreted extracellularly upon proteolytic cleavage at the juxtamembrane site, it is substantially underexpressed in luminal epithelial cells (Bascom et al., 2005; Hirai et al., 1998). In contrast, syntaxin4 is ubiquitously and abundantly detectable in a wide variety of epithelial cell types (Bennett et al., 1993; Ding et al., 2018) and lacks a cleavage site for secretion (Hirai et al., 2007). Although this protein undoubtedly exists on the cytoplasmic surface of the plasma membrane as a t-SNARE protein and temporarily forms unique protein complexes with certain cytoplasmic components for intravesicular fusion

Journal of Cell Science (2021) 134, jcs258905. doi:10.1242/jcs.258905

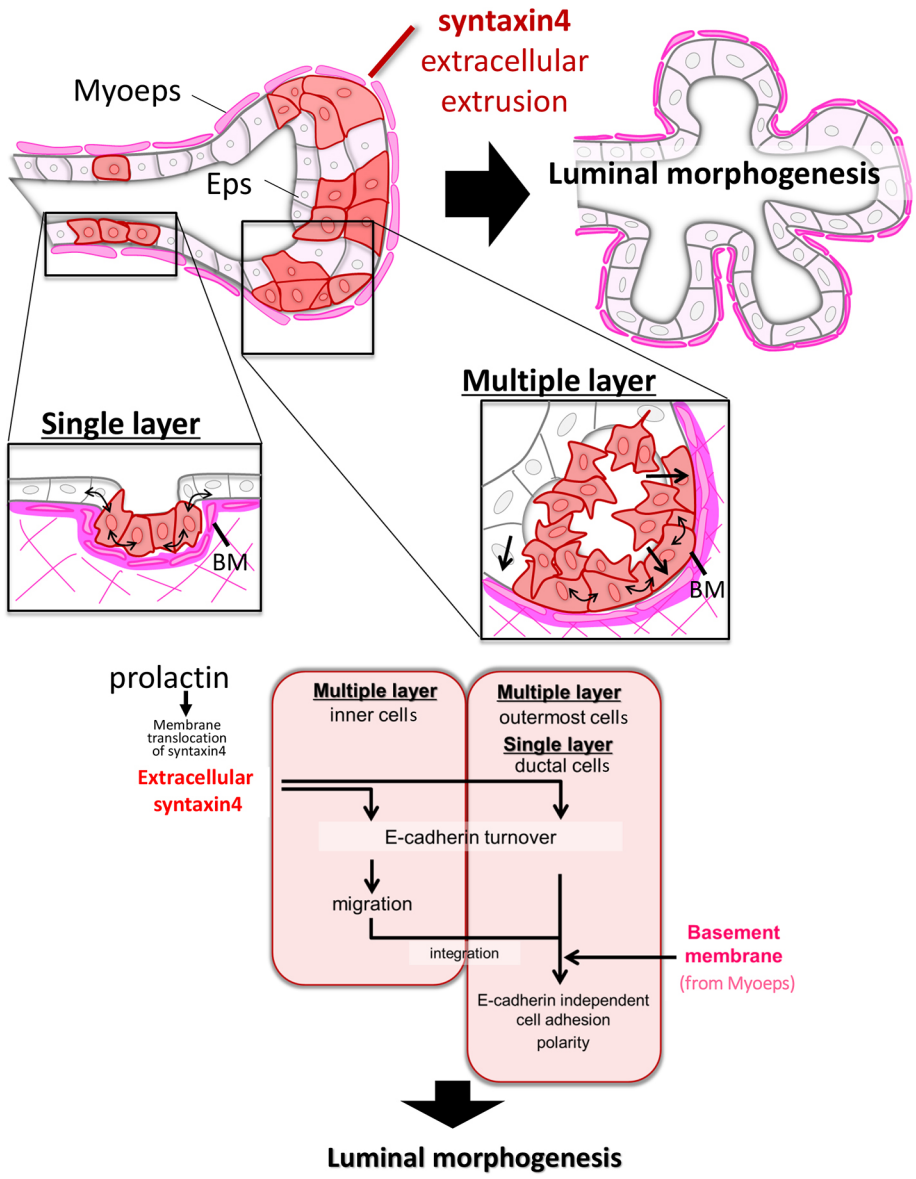

Fig. 8. Schematic diagram of a model for functional coordination of mammary epithelial morphogenesis by syntaxin4 and BM components. In response to the lactogenic hormone prolactin, cells in certain areas of the mammary epithelia (Eps) extrude syntaxin4, which actively triggers E-cadherin turnover and induces dramatic cellular arrangements. Cell populations that are situated away from BM-producing myoepithelial cells (Myoeps), such as at the tip of side branches, actively migrate outward and integrate into the outermost cell layers facing the BM-producing Myoeps. Concurrently, cells in contact with BM-producing Myoeps, such as in the single layered ducts or the outermost cell population in multiple layered Eps, reinforce E-cadherin-independent intercellular adhesion and establish apicobasal polarity to undergo a dramatic cellular arrangement for the formation of well-polarized cystic structures.

(Duan et al., 2020), it would be interesting to investigate whether a subpopulation of syntaxin4 is extruded extracellularly upon external stimuli in these tissues, to exert its latent morphogenic functions. If this is the case, extracellular syntaxin4 might be a critical morphogenic regulator or at least contribute to the development of well-polarized epithelial architectures. To date, the extracellular extrusion with limited secretion of syntaxin4 (Kadono et al., 2012) and its involvement in tissue morphogenesis and/or cell differentiation is evident in the skin epidermis and embryonic stem cells (Hagiwara-Chatani et al., 2017; Hagiwara et al., 2013; Kadono et al., 2015). Attempts to identify signals and molecular elements involved in the membrane translocation of syntaxin4 in these tissues are now underway.

MATERIALS AND METHODS

Mice and mammary glands

Mammary glands were collected from ICR or BALB/C mice (7 weeks of age, pregnancy period day 13, and lactation period day 1) purchased from SLC (Shizuoka, Japan). For whole-mount staining, the glands were fixed with Methacarn solution and stained with Carmine Alum solution (Stem Cell Technologies, Vancouver, Canada), as previously described (Murata et al., 2015). Some glands were fixed with methanol at −20°C, cryosectioned and analyzed using immunohistochemistry. All experiments using mice were approved by the Committee for Animal Experimentation at Kwansei Gakuin University (approval number: 2020-27).

Cells and transfectants

The mouse mammary luminal epithelial cell line EpH4 (gifted by Dr Ernst Reichmann, IMP, Vienna, Austria; Fialka et al., 1996), Madin–Darby canine kidney cell line MDCK II (CRL2936 from ATCC) and mouse fibroblast cell line L and its derivative EL (gifted by Dr Masatoshi Takeichi, RIKEN, Kobe, Japan; Nagafuchi et al., 1987) were maintained in DMEM/Ham's F12 medium (Wako, Japan) supplemented with 10% fetal bovine serum (FBS; MP Bio, Tokyo, Japan) and penicillin and streptomycin (Meiji, Tokyo, Japan) (referred to here as DH10). Cells with a tetracycline-repressive expression system were maintained in DH10 supplemented with 5 µg/ml tetracycline (tet). To generate cells with tet-regulated T7-tagged syntaxin4, or T7-tagged syntaxin4 containing an N-terminal fusion of an exogenous signal peptide from IL-2, cDNA encoding the corresponding polypeptide (Hagiwara-Chatani et al., 2017) was subcloned into a PiggyBac-based tet-regulatable expression plasmid (Woltjen et al., 2009).

Journal of Cell Science (2021) 134, jcs258905. doi:10.1242/jcs.258905

EpH4 cells and EL cells were stably transfected with the generated plasmid together with pTet-TAK (Thermo Fisher Scientific, St Louis, USA), pCAG-PBase (gifted by Dr Yoshiyuki Seki, Kwansei Gakuin University, Hyogo, Japan), and pSV40Neo (gifted by Dr Masatoshi Takeichi, RIKEN, Kobe, Japan) using Lipofectamine 2000 (Invitrogen, St Louis, USA). After G418 selection (0.2 mg/ml), cell clones expressing exogenous syntaxin4 upon removal of tetracycline were isolated and expanded. To knockout the syntaxin4 gene in EpH4 cells, the CRISPR/Cas9 system was used. EpH4 cells were transfected with pSpCas9 BB-2A-Puro plasmid (Addgene, MA, USA) in which one of the annealed DNAs (target-1 positive strand, 5′-CACCGCGACAGGACCCACGAGTTG-3′; target-1 negative strand, 5′-AAACCAACTCGTGGGTCCTGTCGC-3′; target-2 positive strand, 5′-CACCGTGGGTCCTGTCGCGCATGG-3′; target-2 negative strand, 5′-AAACCCATGCGCGGACAGGACCCAC-3′) was inserted into BbsI restriction sites, selected using puromycin-containing DH10, cloned, and tested for complete ablation of syntaxin4 expression. Because the sequence of target-2 contained the syntaxin4 5′-UTR, cells generated using this target (clone 2) could re-express syntaxin4 by introduction of the syntaxin4 expression cassette containing only the syntaxin4-coding region.

Reagents for cell treatment

Prolactin was purchased from Sigma-Aldrich and was added to some cultures at a concentration of 3 µg/ml, along with 1 µg/ml hydrocortisone (Wako, Tokyo), which reportedly improves the organization of organelles (Mills and Topper, 1970). Some cells were labeled with a lipophilic carbocyanine dye, DiO (Thermo Fisher Scientific, St Louis, MO, USA), following the manufacturer's protocol. Chloroquine, an inhibitor of lysosome degradation (Sigma-Aldrich, St Louis, USA) was dissolved in phosphate-buffered saline (PBS) and used at concentrations of 50 or 100 µM. A pan-caspase inhibitor, ZVAD-FMK (Selleck, Tokyo, Japan) and a selective proteasome inhibitor, lactacystin (Abcam, Cambridge, UK), were dissolved in DMSO and used at a concentration of 20 µM and 10 µM, respectively.

Three-dimensional culture

Cells (2.0×10^5/500 µl) were seeded in each well of a 24-well plate, the bottom of which was pre-coated with 1% agarose gel, and then rotated at 100 rpm for 24 h at 37°C, resulting in the formation of well-rounded cell aggregates, as previously described (Hirai et al., 1998). The cell aggregates were then collected, suspended in ice-cold Matrigel (Corning, NY, USA), seeded in 96-well plates, and incubated at 37°C. After gelation, DH10 medium with (syntaxin4 OFF) or without (syntaxin4 ON) 5 µg/ml tetracycline was added to each well.

Transcriptional analysis

Total RNA was extracted using a Total RNA Extraction Miniprep system (VIOGENE, USA) and reverse-transcribed using an RNA-PCR kit (Takara, Shiga, Japan). Quantitative real-time PCR (qRT-PCR) was performed using Fast Start Essential DNA Green Master on a Right Cycler Nano system (Roche, Basel, Switzerland). The cDNAs were amplified using primer pairs for *MMP-3* (5′-TGCAGCTCTACTTTGTTCTTTGA-3′ and 5′-AGAGA-TTTGCGCCAAAAGTG-3′) and *MMP-9* (5′-AGACGACATAGACGG-CATCC-3′ and 5′-TCGGCTGTGGTTCAGTTGT-3′). The relative expression of mRNA was normalized to that of *GAPDH*. To determine the transcriptional profiles of cells with and without syntaxin4, and on collagen and Matrigel, total RNA was extracted as described above, and RNA-sequencing analysis was outsourced to Macrogen Japan Corp. (Tokyo, Japan), which successfully processed data on 13,095 genes in a single experiment. To analyze the molecular elements of EMT-like cell behaviors, all genes encoding keratins and MMPs in the Gene Ontology terms ‘keratin’ (11 genes) and ‘MMP’ (13 genes) that exhibited substantial changes in expression compared to the comparative group (more than 1.5-fold) were extracted and listed. To analyze the molecular elements regulated by the synergistic effects of syntaxin4 and Matrigel, all genes in the word categories ‘cell–cell adhesion’ and ‘apical/basal part of the cells’ that exhibited substantial expression changes between syntaxin4-expressing cells (Sig–Stx4 ON) cultured on Matrigel and on the collagen control were listed (65 genes from the former, and 31 genes from the latter). The six (for cell–cell adhesion) or seven (for apical/basal part of the cells) genes at the top of the list showing the profound upregulation in the cells on Matrigel were extracted, and the expression of these genes was further analyzed in the data from cells without syntaxin4 (Sig–Stx4 OFF) but with Matrigel.

Immunodetection

Antibodies used for experiments included those against β-actin (A3854 from Sigma-Aldrich, St Louis, USA) at 1:5000 dilution, alpha-tubulin (T9026 from Sigma-Aldrich, St Louis, USA) at 1:1000 dilution, T7-tag (PM022 from MBL Life Science, Tokyo, Japan) at 1:1000 dilution, and caspase-3 (9664S from Cell Signaling Technology, MA., USA) at 1:1000 dilution. Monoclonal antibodies against E-cadherin and ZO-1 were gifted by Drs Takeichi (RIKEN, Kobe, Japan) and Nagafuchi (Nara Medical University, Nara, Japan), respectively. Immunoblot analysis was performed according to standard procedures, and immunohistochemistry and immunocytochemistry were performed using the following protocol. Cell aggregates were fixed with 4% paraformaldehyde (PFA) in Tris-buffered saline (TBS) for 1 h and permeabilized with 0.5% Triton X-100 for 30 min. Cells cultured on dishes were fixed with 4% PFA in TBS for 10 min and permeabilized with 0.1% Triton X-100 for 10 min. Each sample was then incubated with 5% FBS for 1 h, primary antibody overnight, and labeled with secondary antibodies for 2 h, followed by extensive washing with TBS at each interval. Nuclei were counterstained with DAPI (Sigma-Aldrich, St Louis, USA). Samples were mounted on glass slides and analyzed using an A1 confocal microscope system (Nikon, Tokyo, Japan) or Leica TCS SPE (Leica, Wetzlar, Germany) with 20×, 40× or 60× objectives.

Detection of proteins expressed at the cell surface

To detect extracellularly expressed proteins in EpH4 cells, living cells cultured in Transwell chambers (1.0 µm in diameter; Costar, NY, USA) were washed with PBS and treated with 0.1 mg/ml Sulfo-NHS-SS biotin (Thermo Fisher Scientific, MA, USA) in PBS from both apical (0.5 ml) and basal (1 ml) sides for 30 min. After washing with DH10 several times to inactivate the NHS group in the residual NHS-SS-biotin, cells were lysed in lysis buffer (1%Triton-X100 and 1% NP-40 in TBS). Biotinylated cell surface proteins were then retrieved with NeutrAvidin beads (Thermo Fisher Scientific, MA, USA) and analyzed by immunoblotting.

Cell fraction insolubilized in cell lysis buffer

Cells treated with lysis buffer were centrifuged at 9,500 ***g*** for 15 min, and the resultant supernatant and pellet were treated as the soluble and insoluble fractions, respectively.

Time-lapse imaging

Cell migratory behavior in the aggregates was analyzed by recording microscopic images every 60 min for 5 days using a Cellwatcher (Corefront, Tokyo, Japan). Time-lapse movies were obtained from the recorded images.

Ultrastructural analyses

To determine the ultrastructural characteristics of cysts induced by extracellular syntaxin4, the cultured samples with and without tetracycline were treated with 2% glutaraldehyde in PBS. These samples were sent to the Hanaichi Ultrastructure Research Institute (Aichi, Japan) to obtain transmission electron microscopy images.

Dissociation assay for instantaneous cell–cell adhesion mediated by E-cadherin

To determine the instantaneous cell adhesive properties of EL cells, we conducted a dissociation assay according to an established protocol (Nagafuchi et al., 1994). EL cells that had been introduced with tet-regulatable expression plasmid for extracellular syntaxin4 were pre-cultured for three days with or without tetracycline. These cells were then treated with 0.01% trypsin for 20 min in HEPES-buffered saline containing 2 mM $CaCl_2$, dissociated by passing through a pipette tip ten times, and the

number of dissociated single cells and the size of the undissociated cell aggregates were analyzed. Parental L cells were used as a control.

Statistical analyses

Results are expressed as the mean±s.d. from at least three independent experiments. Data were analyzed by a two-tailed, paired Student's *t*-test, and a *P*-value of <0.05 was considered statistically significant.

Acknowledgements

We thank Drs Takeichi and Nagafuchi for EL cells and antibodies against E-cadherin (ECCD2) and ZO-1. We are grateful to all members of Hirai laboratory for helpful discussions.

Competing interests

The authors declare no competing or financial interests.

Author contributions

Conceptualization: Y. Hirose, Y. Hirai; Methodology: Y. Hirose; Validation: Y. Hirai; Formal analysis: Y. Hirose; Investigation: Y. Hirose; Resources: Y. Hirai; Data curation: Y. Hirose, Y. Hirai; Writing - original draft: Y. Hirose, Y. Hirai; Writing - review & editing: Y. Hirai; Supervision: Y. Hirai; Funding acquisition: Y. Hirai.

Funding

Part of this work was supported by Grants-in Aid for Scientific Research from the Japan Society for the Promotion of Science (19J22142 to Y. Hirose, 17K09739 to Y. Hirai) and by the Kwansei Gakuin University Special Research Fund (167AB0177a to Y. Hirai).

Data availability

RNA-seq read count data are available from the Dryad Digital Repository (Hirose and Hirai, 2021): https://doi.org/10.5061/dryad.12jm63z05.

Peer review history

The peer review history is available online at https://journals.biologists.com/jcs/article-lookup/doi/10.1242/jcs.258905.

References

Akhtar, N. and Streuli, C. H. (2013). An integrin-ILK-microtubule network orients cell polarity and lumen formation in glandular epithelium. *Nat. Cell Biol.* **15**, 17-27. doi:10.1038/ncb2646

Bascom, J. L., Fata, J. E., Hirai, Y., Sternlicht, M. D. and Bissell, M. J. (2005). Epimorphin overexpression in the mouse mammary gland promotes alveolar hyperplasia and mammary adenocarcinoma. *Cancer Res.* **65**, 8617-8621. doi:10.1158/0008-5472.CAN-05-1985

Bennett, M. K., Garcia-Arrarás, J. E., Elferink, L. A., Peterson, K., Fleming, A. M., Hazuka, C. D. and Scheller, R. H. (1993). The syntaxin family of vesicular transport receptors. *Cell* **74**, 863-873. doi:10.1016/0092-8674(93)90466-4

Bolander, F. F.Jr. (1985). Possible roles of calcium and calmodulin in mammary gland differentiation in vitro. *J. Endocrinol.* **104**, 29-34. doi:10.1677/joe.0.1040029

Brisken, C. and O'Malley, B. (2010). Hormone action in the mammary gland. *Cold Spring Harb. Perspect. Biol.* **2**, a003178. doi:10.1101/cshperspect.a003178

Brüser, L. and Bogdan, S. (2017). Adherens junctions on the move-membrane trafficking of e-cadherin. *Cold Spring Harb. Perspect. Biol.* **9**, a029140. doi:10.1101/cshperspect.a029140

Bryant, D. M., Datta, A., Rodríguez-Fraticelli, A. E., Peränen, J., Martín-Belmonte, F. and Mostov, K. E. (2010). A molecular network for de novo generation of the apical surface and lumen. *Nat. Cell Biol.* **12**, 1035-1045. doi:10.1038/ncb2106

Bryant, D. M., Roignot, J., Datta, A., Overeem, A. W., Kim, M., Yu, W., Peng, X., Eastburn, D. J., Ewald, A. J., Werb, Z. et al. (2014). A molecular switch for the orientation of epithelial cell polarization. *Dev. Cell* **31**, 171-187. doi:10.1016/j.devcel.2014.08.027

Burgoyne, R. D., Handel, S. E., Morgan, A., Rennison, M. E., Turner, M. D. and Wilde, C. J. (1991). Calcium, the cytoskeleton and calpactin (annexin II) in exocytotic secretion from adrenal chromaffin and mammary epithelial cells. *Biochem. Soc. Trans.* **19**, 1085-1090. doi:10.1042/bst0191085

Campbell, K. and Casanova, J. (2016). A common framework for EMT and collective cell migration. *Development* **143**, 4291-4300. doi:10.1242/dev.139071

Chen, W. C. and Obrink, B. (1991). Cell-cell contacts mediated by E-cadherin (uvomorulin) restrict invasive behavior of L-cells. *J. Cell Biol.* **114**, 319-327. doi:10.1083/jcb.114.2.319

Chen, Q. K., Lee, K. A., Radisky, D. C. and Nelson, C. M. (2013). Extracellular matrix proteins regulate epithelial-mesenchymal transition in mammary epithelial cells. *Differentiation* **86**, 126-132. doi:10.1016/j.diff.2013.03.003

Debnath, J. and Brugge, J. S. (2005). Modelling glandular epithelial cancers in three-dimensional cultures. *Nat. Rev. Cancer* **5**, 675-688. doi:10.1038/nrc1695

Debnath, J., Mills, K. R., Collins, N. L., Reginato, M. J., Muthuswamy, S. K. and Brugge, J. S. (2002). The role of apoptosis in creating and maintaining luminal space within normal and oncogene-expressing mammary acini. *Cell* **111**, 29-40. doi:10.1016/S0092-8674(02)01001-2

Ding, C., Cong, X., Zhang, Y., Li, S.-L., Wu, L.-L. and Yu, G.-Y. (2018). β-adrenoceptor activation increased VAMP-2 and syntaxin-4 in secretory granules are involved in protein secretion of submandibular gland through the PKA/F-actin pathway. *Biosci. Rep.* **38**, BSR20171142. doi:10.1042/BSR20171142

Druso, J. E., Endo, M., Lin, M.-C. J., Peng, X., Antonyak, M. A., Meller, S. and Cerione, R. A. (2016). An essential role for Cdc42 in the functioning of the adult mammary gland. *J. Biol. Chem.* **291**, 8886-8895. doi:10.1074/jbc.M115.694349

Duan, X.-L., Guo, Z., He, Y.-T., Li, Y.-X., Liu, Y.-N., Bai, H.-H., Li, H.-L., Hu, X.-D. and Suo, Z.-W. (2020). SNAP25/syntaxin4/VAMP2/Munc18-1 complexes in spinal dorsal horn contributed to inflammatory pain. *Neuroscience* **429**, 203-212. doi:10.1016/j.neuroscience.2020.01.003

Dumortier, J. G., Le Verge-Serandour, M., Tortorelli, A. F., Mielke, A., de Plater, L., Turlier, H. and Maître, J.-L. (2019). Hydraulic fracturing and active coarsening position the lumen of the mouse blastocyst. *Science* **365**, 465-468. doi:10.1126/science.aaw7709

Ewald, A. J., Brenot, A., Duong, M., Chan, B. S. and Werb, Z. (2008). Collective epithelial migration and cell rearrangements drive mammary branching morphogenesis. *Dev. Cell* **14**, 570-581. doi:10.1016/j.devcel.2008.03.003

Ewald, A. J., Huebner, R. J., Palsdottir, H., Lee, J. K., Perez, M. J., Jorgens, D. M., Tauscher, A. N., Cheung, K. J., Werb, Z. and Auer, M. (2012). Mammary collective cell migration involves transient loss of epithelial features and individual cell migration within the epithelium. *J. Cell Sci.* **125**, 2638-2654. doi:10.1242/jcs.096875

Fialka, I., Schwarz, H., Reichmann, E., Oft, M., Busslinger, M. and Beug, H. (1996). The estrogen-dependent c-JunER protein causes a reversible loss of mammary epithelial cell polarity involving a destabilization of adherens junctions. *J. Cell Biol.* **132**, 1115-1132. doi:10.1083/jcb.132.6.1115

Friedl, P. and Mayor, R. (2017). Tuning collective cell migration by cell–cell junction regulation. *Cold Spring Harb. Perspect. Biol.* **9**, a029199. doi:10.1101/cshperspect.a029199

Fukata, M., Kuroda, S., Nakagawa, M., Kawajiri, A., Itoh, N., Shoji, I., Matsuura, Y., Yonehara, S., Fujisawa, H., Kikuchi, A. et al. (1999). Cdc42 and Rac1 regulate the interaction of IQGAP1 with beta-catenin. *J. Biol. Chem.* **274**, 26044-26050. doi:10.1074/jbc.274.37.26044

Georgiou, M., Marinari, E., Burden, J. and Baum, B. (2008). Cdc42, Par6, and aPKC regulate Arp2/3-mediated endocytosis to control local adherens junction stability. *Curr. Biol.* **18**, 1631-1638. doi:10.1016/j.cub.2008.09.029

Gudjonsson, T., Adriance, M. C., Sternlicht, M. D., Petersen, O. W. and Bissell, M. J. (2005). Myoepithelial cells: their origin and function in breast morphogenesis and neoplasia. *J. Mammary Gland Biol. Neoplasia* **10**, 261-272. doi:10.1007/s10911-005-9586-4

Hagiwara, N., Kadono, N., Miyazaki, T., Maekubo, K. and Hirai, Y. (2013). Extracellular syntaxin4 triggers the differentiation program in teratocarcinoma F9 cells that impacts cell adhesion properties. *Cell Tissue Res.* **354**, 581-591. doi:10.1007/s00441-013-1680-0

Hagiwara-Chatani, N., Shirai, K., Kido, T., Horigome, T., Yasue, A., Adachi, N. and Hirai, Y. (2017). Membrane translocation of t-SNARE protein syntaxin-4 abrogates ground-state pluripotency in mouse embryonic stem cells. *Sci. Rep.* **7**, 39868. doi:10.1038/srep39868

Hinck, L. and Silberstein, G. B. (2005). Key stages in mammary gland development: the mammary end bud as a motile organ. *Breast Cancer Res.* **7**, 245-251. doi:10.1186/bcr1331

Hirai, Y. (2001). Epimorphin as a morphogen: does a protein for intracellular vesicular targeting act as an extracellular signaling molecule? *Cell Biol. Int.* **25**, 193-195. doi:10.1006/cbir.2000.0618

Hirai, Y., Lochter, A., Galosy, S., Koshida, S., Niwa, S. and Bissell, M. J. (1998). Epimorphin functions as a key morphoregulator for mammary epithelial cells. *J. Cell Biol.* **140**, 159-169. doi:10.1083/jcb.140.1.159

Hirai, Y., Takebe, K., Takashina, M., Kobayashi, S. and Takeichi, M. (1992). Epimorphin: a mesenchymal protein essential for epithelial morphogenesis. *Cell* **69**, 471-481. doi:10.1016/0092-8674(92)90448-L

Hirai, Y., Nelson, C. M., Yamazaki, K., Takebe, K., Przybylo, J., Madden, B. and Radisky, D. C. (2007). Non-classical export of epimorphin and its adhesion to {alpha}v-integrin in regulation of epithelial morphogenesis. *J. Cell Sci.* **120**, 2032-2043. doi:10.1242/jcs.006247

Hirose, Y. and Hirai, Y. (2021). Data from: Cooperation of membrane-translocated syntaxin4 and basement membrane for dynamic mammary epithelial morphogenesis. *Dryad Digital Repository*. doi:10.5061/dryad.12jm63z05

Hirose, Y., Shirai, K. and Hirai, Y. (2018). Membrane-tethered syntaxin-4 locally abrogates E-cadherin function and activates Smad signals, contributing to asymmetric mammary epithelial morphogenesis. *J. Cell. Biochem.* **119**, 7525-7539. doi:10.1002/jcb.27064

Ivanova, E., Le Guillou, S., Hue-Beauvais, C. and Le Provost, F. (2021). Epigenetics: new insights into mammary gland biology. *Genes (Basel)* **12**, 231. doi:10.3390/genes12020231

Janda, E., Nevolo, M., Lehmann, K., Downward, J., Beug, H. and Grieco, M. (2006). Raf plus TGFbeta-dependent EMT is initiated by endocytosis and lysosomal degradation of E-cadherin. *Oncogene* **25**, 7117-7130. doi:10.1038/sj.onc.1209701

Kadono, N., Miyazaki, T., Okugawa, Y., Nakajima, K. and Hirai, Y. (2012). The impact of extracellular syntaxin4 on HaCaT keratinocyte behavior. *Biochem. Biophys. Res. Commun.* **417**, 1200-1205. doi:10.1016/j.bbrc.2011.12.107

Kadono, N., Hagiwara, N., Tagawa, T., Maekubo, K. and Hirai, Y. (2015). Extracellularly extruded syntaxin-4 is a potent cornification regulator of epidermal keratinocytes. *Mol. Med.* **21**, 77-86. doi:10.2119/molmed.2014.00234

Kiener, H. P., Niederreiter, B., Lee, D. M., Jimenez-Boj, E., Smolen, J. S. and Brenner, M. B. (2009). Cadherin 11 promotes invasive behavior of fibroblast-like synoviocytes. *Arthritis. Rheum.* **60**, 1305-1310. doi:10.1002/art.24453

Kota, P., Terrell, E. M., Ritt, D. A., Insinna, C., Westlake, C. J. and Morrison, D. K. (2019). M-Ras/Shoc2 signaling modulates E-cadherin turnover and cell-cell adhesion during collective cell migration. *Proc. Natl. Acad. Sci. USA* **116**, 3536-3545. doi:10.1073/pnas.1805919116

Kowalczyk, A. P. and Nanes, B. A. (2012). Adherens junction turnover: regulating adhesion through cadherin endocytosis, degradation, and recycling. *Subcell. Biochem.* **60**, 197-222. doi:10.1007/978-94-007-4186-7_9

Kuroda, S., Fukata, M., Nakagawa, M., Fujii, K., Nakamura, T., Ookubo, T., Izawa, I., Nagase, T., Nomura, N., Tani, H. et al. (1998). Role of IQGAP1, a target of the small GTPases Cdc42 and Rac1, in regulation of E-cadherin- mediated cell-cell adhesion. *Science* **281**, 832-835. doi:10.1126/science.281.5378.832

Lamouille, S., Xu, J. and Derynck, R. (2014). Molecular mechanisms of epithelial–mesenchymal transition. *Nat. Rev. Mol. Cell Biol.* **15**, 178-196. doi:10.1038/nrm3758

Lehnert, L., Lerch, M. M., Hirai, Y., Kruse, M.-L., Schmiegel, W. and Kalthoff, H. (2001). Autocrine stimulation of human pancreatic duct-like development by soluble isoforms of epimorphin in vitro. *J. Cell Biol.* **152**, 911-922. doi:10.1083/jcb.152.5.911

Leibfried, A., Fricke, R., Morgan, M. J., Bogdan, S. and Bellaiche, Y. (2008). Drosophila Cip4 and WASp define a branch of the Cdc42-Par6-aPKC pathway regulating E-cadherin endocytosis. *Curr. Biol.* **18**, 1639-1648. doi:10.1016/j.cub.2008.09.063

Macias, H. and Hinck, L. (2012). Mammary gland development. *Wiley Interdiscip. Rev. Dev. Biol.* **1**, 533-557. doi:10.1002/wdev.35

Martín-Belmonte, F., Yu, W., Rodríguez-Fraticelli, A. E., Ewald, A. J., Werb, Z., Alonso, M. A. and Mostov, K. (2008). Cell-polarity dynamics controls the mechanism of lumen formation in epithelial morphogenesis. *Curr. Biol.* **18**, 507-513. doi:10.1016/j.cub.2008.02.076

Meng, W., Mushika, Y., Ichii, T. and Takeichi, M. (2008). Anchorage of microtubule minus ends to adherens junctions regulates epithelial cell-cell contacts. *Cell* **135**, 948-959. doi:10.1016/j.cell.2008.09.040

Mills, E. S. and Topper, Y. J. (1970). Some ultrastructural effects of insulin, hydrocortisone, and prolactin on mammary gland explants. *J. Cell Biol.* **44**, 310-328. doi:10.1083/jcb.44.2.310

Murata, K., Baasanjav, A., Kwon, C., Hashimoto, M., Ishida, J. and Fukamizu, A. (2015). Angiotensin II accelerates mammary gland development independently of high blood pressure in pregnancy-associated hypertensive mice. *Physiol. Rep.* **3**, e12542. doi:10.14814/phy2.12542

Nagafuchi, A., Shirayoshi, Y., Okazaki, K., Yasuda, K. and Takeichi, M. (1987). Transformation of cell adhesion properties by exogenously introduced E-cadherin cDNA. *Nature* **329**, 341-343. doi:10.1038/329341a0

Nagafuchi, A., Ishihara, S. and Tsukita, S. (1994). The roles of catenins in the cadherin-mediated cell adhesion: functional analysis of E-cadherin-alpha catenin fusion molecules. *J. Cell Biol.* **127**, 235-245. doi:10.1083/jcb.127.1.235

Neumann, N. M., Perrone, M. C., Veldhuis, J. H., Huebner, R. J., Zhan, H., Devreotes, P. N., Brodland, G. W. and Ewald, A. J. (2018). Coordination of receptor tyrosine kinase signaling and interfacial tension dynamics drives radial intercalation and tube elongation. *Dev. Cell* **45**, 67-82.e6. doi:10.1016/j.devcel.2018.03.011

Okugawa, Y. and Hirai, Y. (2008). Overexpression of extracellular epimorphin leads to impaired epidermal differentiation in HaCaT keratinocytes. *J. Invest. Dermatol.* **128**, 1884-1893. doi:10.1038/jid.2008.22

Paine, I. S. and Lewis, M. T. (2017). The terminal end bud: the little engine that could. *J. Mammary Gland Biol. Neoplasia* **22**, 93-108. doi:10.1007/s10911-017-9372-0

Radisky, D. C., Stallings-Mann, M., Hirai, Y. and Bissell, M. J. (2009). Single proteins might have dual but related functions in intracellular and extracellular microenvironments. *Nat. Rev. Mol. Cell Biol.* **10**, 228-234. doi:10.1038/nrm2633

Roignot, J., Peng, X. and Mostov, K. (2013). Polarity in mammalian epithelial morphogenesis. *Cold Spring Harb. Perspect. Biol.* **5**, a013789. doi:10.1101/cshperspect.a013789

Sako-Kubota, K., Tanaka, N., Nagae, S., Meng, W. and Takeichi, M. (2014). Minus end-directed motor KIFC3 suppresses E-cadherin degradation by recruiting USP47 to adherens junctions. *Mol. Biol. Cell* **25**, 3851-3860. doi:10.1091/mbc.e14-07-1245

Shamir, E. R. and Ewald, A. J. (2015). Adhesion in mammary development: novel roles for e-cadherin in individual and collective cell migration. *Curr. Top. Dev. Biol.* **112**, 353-382. doi:10.1016/bs.ctdb.2014.12.001

Shirai, K., Hagiwara, N., Horigome, T., Hirose, Y., Kadono, N. and Hirai, Y. (2017). Extracellularly extruded syntaxin-4 binds to laminin and syndecan-1 to regulate mammary epithelial morphogenesis. *J. Cell. Biochem.* **118**, 686-698. doi:10.1002/jcb.25661

Smoczyński, M. (2017). Role of phospholipid flux during milk secretion in the mammary gland. *J. Mammary Gland Biol. Neoplasia* **22**, 117-129. doi:10.1007/s10911-017-9376-9

Song, S., Eckerle, S., Onichtchouk, D., Marrs, J. A., Nitschke, R. and Driever, W. (2013). Pou5f1-dependent EGF expression controls E-cadherin endocytosis, cell adhesion, and zebrafish epiboly movements. *Dev. Cell* **24**, 486-501. doi:10.1016/j.devcel.2013.01.016

Sternlicht, M. D., Kouros-Mehr, H., Lu, P. and Werb, Z. (2006). Hormonal and local control of mammary branching morphogenesis. *Differentiation* **74**, 365-381. doi:10.1111/j.1432-0436.2006.00105.x

Takeichi, M. (2014). Dynamic contacts: rearranging adherens junctions to drive epithelial remodelling. *Nat. Rev. Mol. Cell Biol.* **15**, 397-410. doi:10.1038/nrm3802

Vidi, P.-A., Bissell, M. J. and Lelièvre, S. A. (2013). Three-dimensional culture of human breast epithelial cells: the how and the why. *Methods Mol. Biol.* **945**, 193-219. doi:10.1007/978-1-62703-125-7_13

Woltjen, K., Michael, I. P., Mohseni, P., Desai, R., Mileikovsky, M., Hämäläinen, R., Cowling, R., Wang, W., Liu, P., Gertsenstein, M. et al. (2009). piggyBac transposition reprograms fibroblasts to induced pluripotent stem cells. *Nature* **458**, 766-770. doi:10.1038/nature07863

Zhang, M., Chen, D., Zhen, Z., Ao, J., Yuan, X. and Gao, X. (2018). Annexin A2 positively regulates milk synthesis and proliferation of bovine mammary epithelial cells through the mTOR signaling pathway. *J. Cell. Physiol.* **233**, 2464-2475. doi:10.1002/jcp.26123

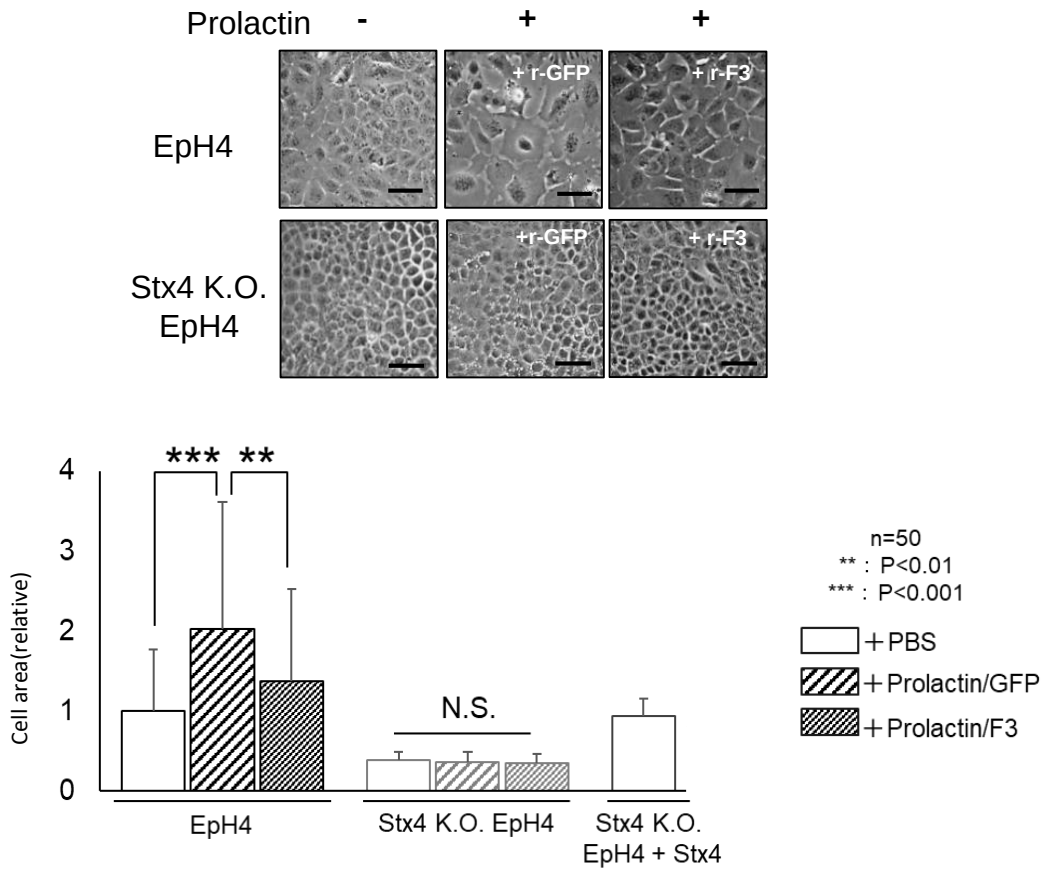

Fig. S1. Prolactin induced flattened morphology in parent EpH4 cells, but not in Stx4 K.O. EpH4 cells, which was blocked by the addition of membrane-impermeable syntaxin4 antagonist r-F3 (Hirose et al., 2017), but not of r-GFP control (50 µg/ml). As Stx4 K.O. clones generated by different gRNAs behaved similarly and exogenous syntaxin4 could be expressed in clone2, the cell size was quantitated only for clone2. Compared to parent EpH4 cells, the size of Stx4 K.O. cells was apparently small, however, re-expression of syntaxin4 recovered the cell size. Bars, 50 µm. Area occupied by a cell is shown. n= 40, ***; $p< 0.001$, **; $p< 0.01$.

	EpH4 +prolactin	T7-Stx4 EpH4 (ON) +prolactin	Sig-T7-Stx4 EpH4(ON)
Cells with extracellular syntaxin-4	partial	partial	total
phenotype	multiple lumen	multiple lumen	single lumen

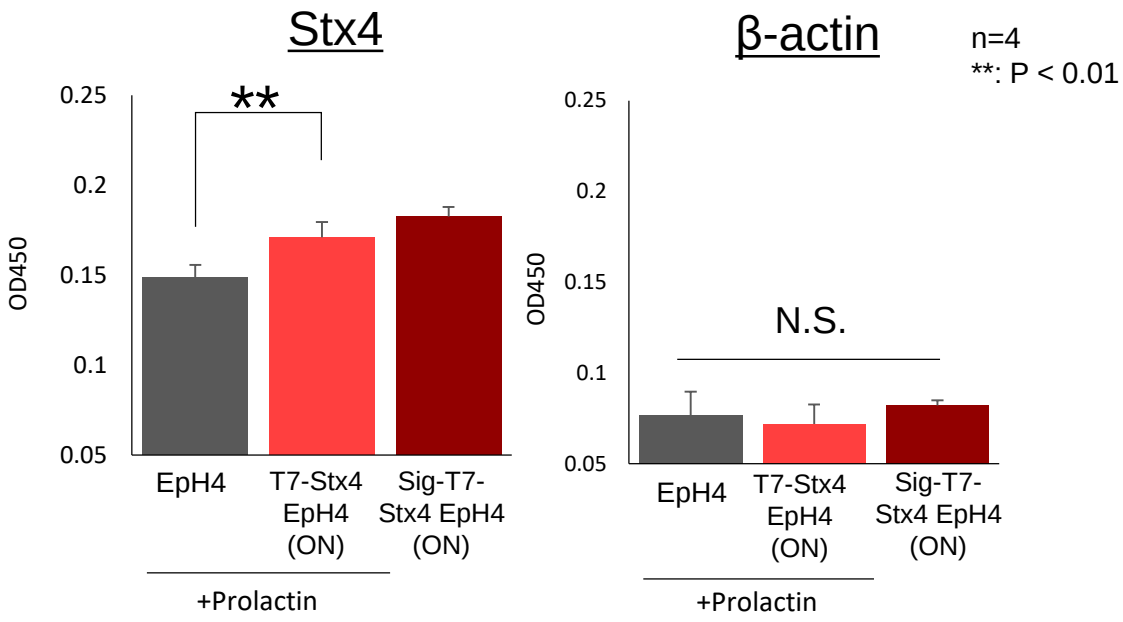

Fig. S2. Upper, the relationship between the mode of expression of extracellular syntaxin-4 and the phenotype. Lower, amount of extracellular syntaxin4 (Stx4) in parental EpH4 cells with prolactin, T7-Stx4 EpH4 cells (ON) with prolactin, and Sig-T7 Stx4 EpH4 cells (ON) without prolactin. Non-permeabilized cells in 96-well plate were incubated with primary antibody against syntaxin4 or β-actin, and with HRP-conjugated secondary antibodies. After excessive washing with TBS, amount of syntaxin4 or β-actin on the cell surface was quantified with TMB solution (Scy Tek, UT, USA) using the plate leader (Thermo Scientific, Finland) . n = 4. **: P < 0.01. As the signal intensity of syntaxin4 in the permeabilized cells is weaker than or similar to that of β-actin (Fig 1B), the lower left graph reflects the expression amount of extracellular syntaxin4.

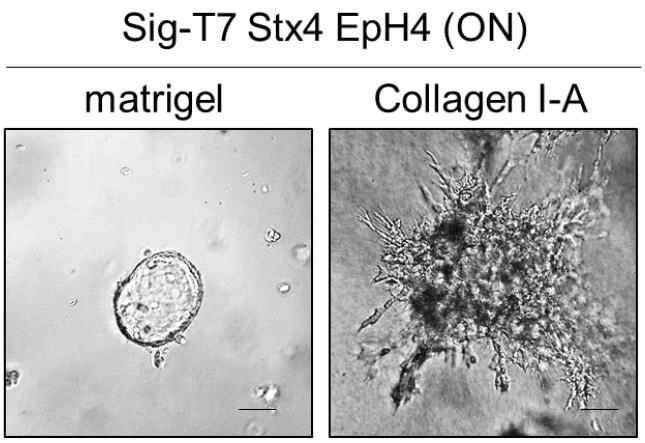

Fig. S3. Sig-T7 Stx4 EpH4 cell aggregates with extracellular syntaxin-4 (ON) were embedded in Matrigel or collagen I and compared the morphological appearance on day 5. In collagen gel Sig-T7 Stx4 EpH4 cells scattered/disseminated and never underwent luminal morphogenesis.

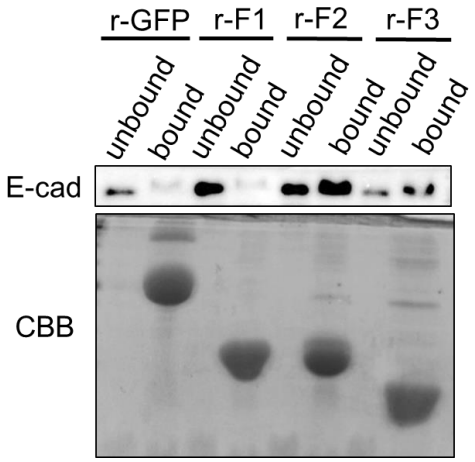

Fig. S4. Syntaxin4 binds to E-cadherin in EpH4 cells via its central and membrane proximal domain. Syntaxin4 fragments (r-F1:Met1-Glu110, r-F2:Ala111-Arg197, r-F3:Glu198-Lys272) tagged with 6X histidine residues were prepared, trapped to Ni-NTA agarose beads, and incubated with EpH4 cell lysate. Unbound and bound materials to the beads were collected and analyzed for E-cadherin by immunoblotting (upper). Equivalent amount of each fragment on the beads was apparent, as judged by Coomassie Brilliant Blue (CBB) staining (lower). The central domain (F2) and membrane proximal domain (F3) bound to E-cadherin expressed in EpH4 cells.

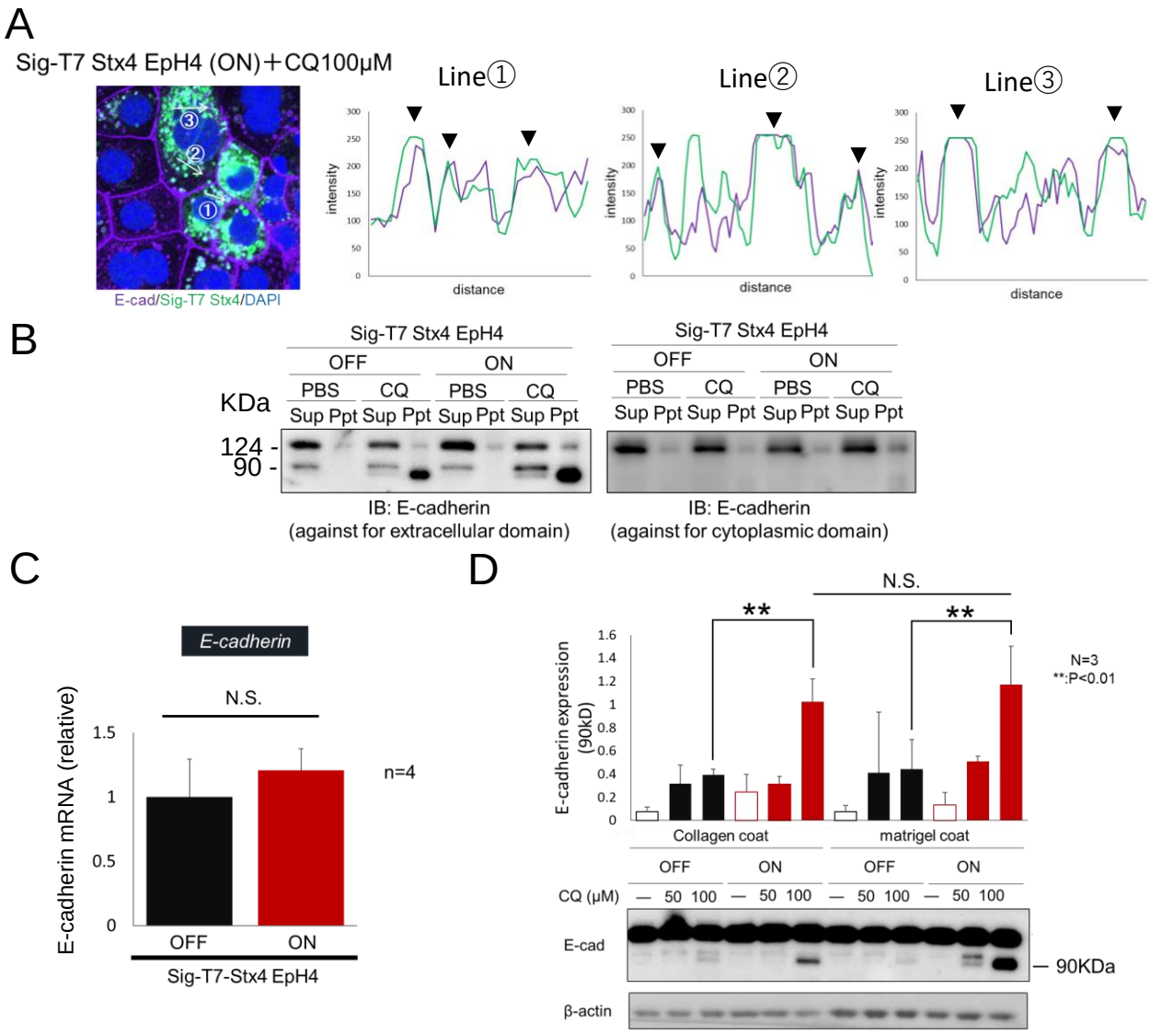

Fig. S5. A, Line scan analyses of E-cadherin (magenta) and sig-T7-Stx4 (green) in sig-T7-Stx4 EpH4 (ON) treated with CQ (same as a lower panel in Fig. 6E). Signal intensities of E-cadherin and sig-T7-Stx4 were analyzed along lines ①, ②, ③ using imageJ. Overlap of each maximum signal intensity shows co-localization of E-cadherin and sig-T7-Stx4 (triangles). B, The 90 kDa form of E-cadherin lacks cytoplasmic tail for cytoskeletal linkage. A monoclonal antibody against extracellular domain of E-cadherin (ECCD2) bound both the full length and the 90 kDa form of E-cadherin, whereas polyclonal antibodies against the cytoplasmic tail (Takara, Japan) failed to recognize the latter. **C**, Expression of extracellular syntaxin4 for 3 days did not affect the expression of E-cadherin mRNA in EpH4 cells. n= 4. D, Signals from Matrigel did not affect the generation of 90 kDa E-cadherin. Sig-T7 Stx4 EpH4 cells on Matrigel or collagen I were treated with various amount of CQ, then the expression of E-cadherin was analyzed. These cells produced 90kDa E-cadherin in response to extracellular syntaxin4 even on Matrigel. N= 3, **; p< 0.01.

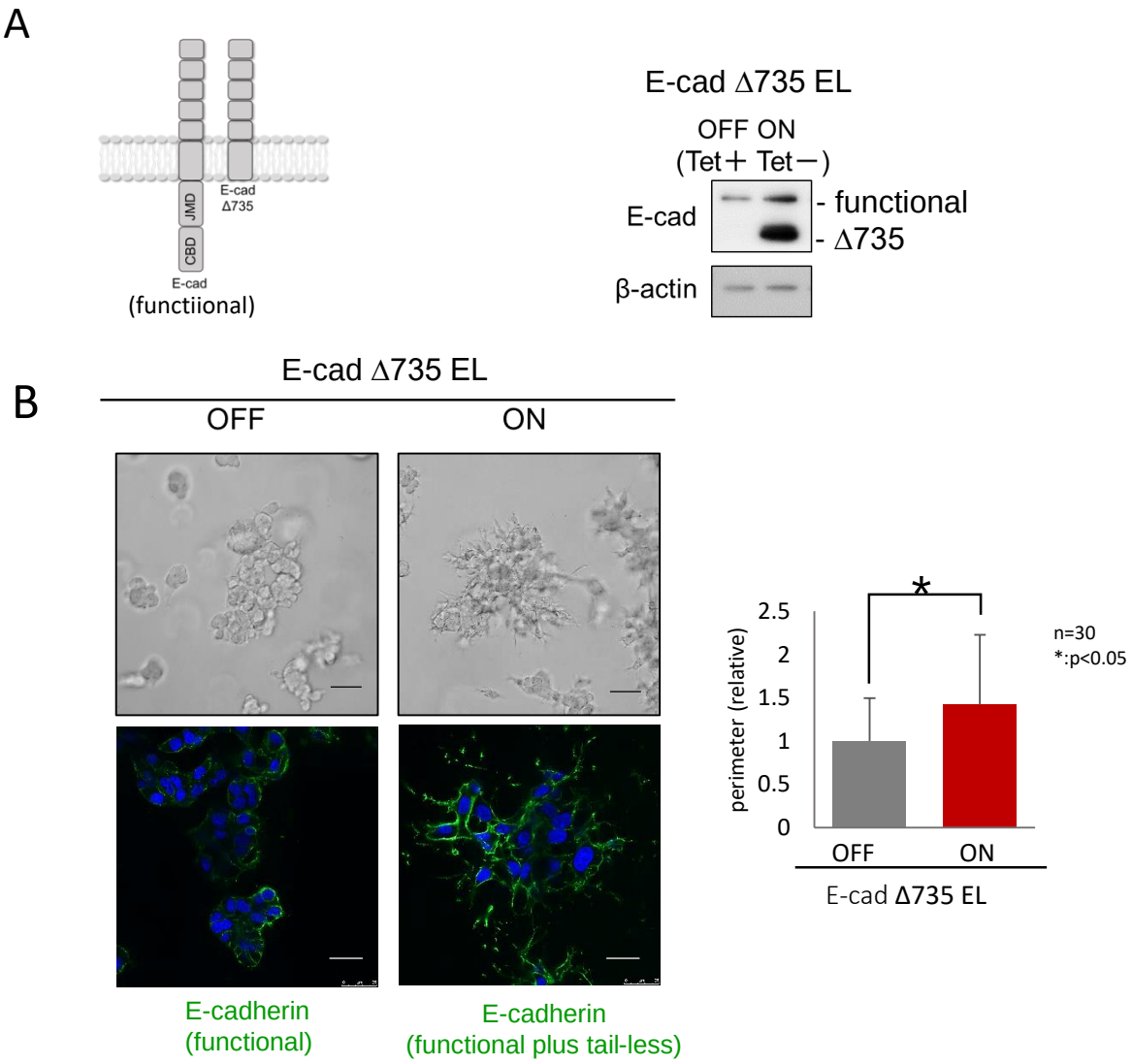

Fig. S6. A, Left, a schematic image of full length (functional) and "tailless" E-cadherin-mutant (E-cad Δ735: Met1~Arg735). Right, EL cells with inducible expression of "tailless" E-cadherin-mutant (E-cadΔ735 EL). EL cells were stably transfected with the PiggyBac-based tet-regulatable expression plasmid containing cDNA for Met1-Arg735 in *E-cadherin* (NCBI 12550). Upon removal of tetracycline (ON), these cells expressed "tailless" E-cadherin-mutant without affecting the amount of functional E-cadherin. B, Left, microscopy images and distribution of E-cadherin in E-cadΔ735 EL cell aggregates embedded in Matrigel for three days. Bars, 50 μm (upper) and 25 μm (lower). Right, quantification of the perimeter of the cell aggregates. n= 30, *; p< 0.05. Cell aggregates with only functional E-cadherin remained as cell clumps, whereas those additionally with E-cadΔ735 were dissociated and scattered.

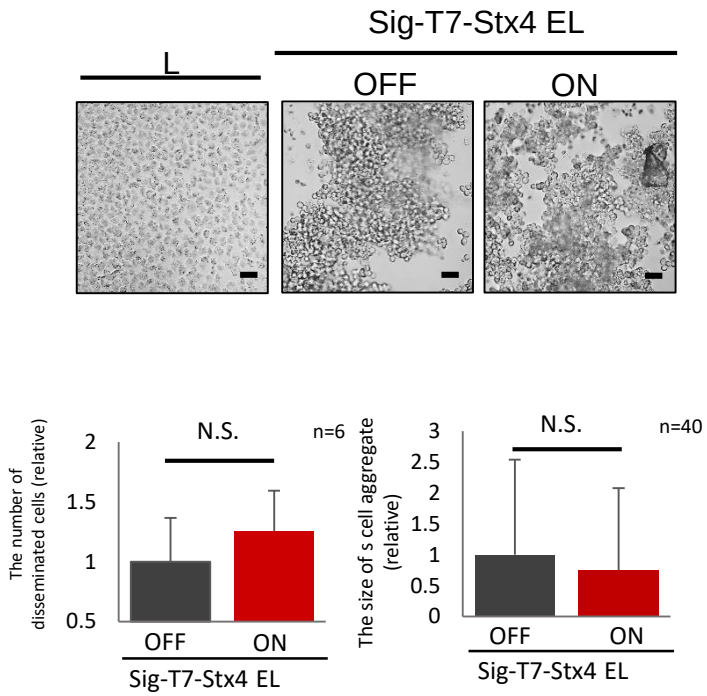

Fig. S7. Upper, light microscopy images of sig-T7-Stx4-EL cells with (ON) and without (OFF) extracellular expression of syntaxin4 in the cell dissociation assay. L cells that have no cadherins were completely dissociated by this treatment. Bars, 50 µm. Lower, relative number of dissociated single cells (left, n= 6), and the size of the undissociated cell aggregates (right, n= 40) after treatment with trypsin in the presence of Ca^{2+}.

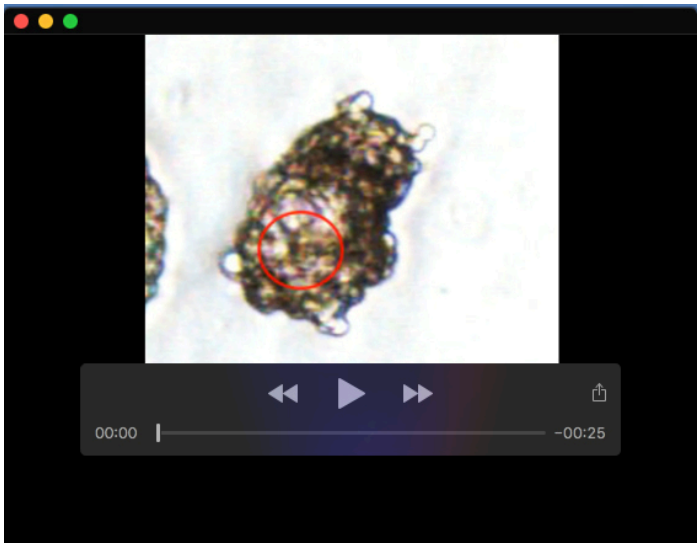

Movie 1. Sig-T7-Stx4 EpH4 aggregates were embedded in Matrigel and time-lapse images was acquired from 48 h of culture and ran for 120 h. Movie was constructed from expanded images from 99 h to 164 h when active cell movement was observed. Red circle indicates the inner cell populations in the aggregate.